



**HAL**  
open science

## Constraining the origin of recently deposited particles using natural radionuclides $^7\text{Be}$ and $^{234}\text{Th}$ in deltaic sediments

Junwen Wu, C. Rabouille, Sabine Charmasson, Jean-Louis Reyss, Xavier Cagnat

► **To cite this version:**

Junwen Wu, C. Rabouille, Sabine Charmasson, Jean-Louis Reyss, Xavier Cagnat. Constraining the origin of recently deposited particles using natural radionuclides  $^7\text{Be}$  and  $^{234}\text{Th}$  in deltaic sediments. *Continental Shelf Research*, 2018, 165, pp.106-119. 10.1016/j.csr.2018.06.010 . hal-02635532

**HAL Id: hal-02635532**

**<https://hal.science/hal-02635532v1>**

Submitted on 27 May 2020

**HAL** is a multi-disciplinary open access archive for the deposit and dissemination of scientific research documents, whether they are published or not. The documents may come from teaching and research institutions in France or abroad, or from public or private research centers.

L'archive ouverte pluridisciplinaire **HAL**, est destinée au dépôt et à la diffusion de documents scientifiques de niveau recherche, publiés ou non, émanant des établissements d'enseignement et de recherche français ou étrangers, des laboratoires publics ou privés.



Distributed under a Creative Commons Attribution - NonCommercial - NoDerivatives 4.0 International License

1

2 **Constraining the origin of recently deposited particles using**  
3 **natural radionuclides  $^7\text{Be}$  and  $^{234}\text{Th}_{\text{ex}}$  in deltaic sediments**

4

5 Junwen Wu<sup>1,2,4</sup>, Christophe Rabouille<sup>2\*</sup>, Sabine Charmasson<sup>1\*</sup>, Jean Louis Reyss<sup>2</sup>, Xavier  
6 Cagnat<sup>3</sup>

7

8 <sup>1</sup>Institut de Radioprotection et de Sûreté Nucléaire (IRSN), PSE-ENV-SRTE Laboratoire  
9 de Recherche sur les Transferts des radionucléides au sein écosystèmes Aquatiques  
10 (LRTA) Centre IFREMER de Méditerranée, CS 20330, zone portuaire de Brégaillon,  
11 83507, La Seyne-sur-Mer Cedex, France

12 <sup>2</sup>Laboratoire des Sciences du Climat et de l'Environnement (LSCE), UMR  
13 CEA/CNRS/UVSQ and IPSL, Avenue de la Terrasse, 91190, Gif-sur-Yvette, France

14 <sup>3</sup>Institut de Radioprotection et de Sûreté Nucléaire (IRSN), PSE-ENV-STEME,  
15 Laboratoire de Mesure de la Radioactivité de l'Environnement (LMRE), Bois des Rames,  
16 91400 Orsay, France

17 <sup>4</sup>College of Science, Shantou University, Shantou 515063, China

18

19

20 **ABSTRACT**

21  $^7\text{Be}$  and  $^{234}\text{Th}_{\text{ex}}$  activities were determined in sediment cores off the Rhône River  
22 mouth (Gulf of Lions), in order to trace the initial transport and deposition of riverine  
23 suspended particulate matter (SPM) and evaluate the impact of flood events through 7  
24 cruises carried out over the period of 2007-2008. Consistently high  $^7\text{Be}$  and  $^{234}\text{Th}_{\text{ex}}$   
25 inventories of 2000-3000 mBq cm<sup>-2</sup> and 3000-5000 mBq cm<sup>-2</sup>, respectively, were  
26 observed within a ~5 km radius off the Rhône River mouth. Their spatial distributions  
27 showed a gradual decrease with increasing distance from the Rhône River mouth, and the  
28 decrease in  $^7\text{Be}$  was more pronounced than that of  $^{234}\text{Th}_{\text{ex}}$ , indicating that recent riverine  
29 SPM is rapidly deposited in the area located near the river mouth. This area is also  
30 characterized by high accumulation rates determined using  $^{137}\text{Cs}$  or  $^{210}\text{Pb}_{\text{ex}}$ . Both  $^7\text{Be}$  and  
31  $^{234}\text{Th}_{\text{ex}}$  inventories increased in 2008 compared to 2007, and are positively correlated to  
32 the cumulated SPM flux for normal and flood discharge. Moreover, the  $^7\text{Be}/^{234}\text{Th}_{\text{ex}}$   
33 inventory ratio appears to be a potential tracer to identify the dominant influence of  
34 recently deposited particles between terrestrial and marine waters. This ratio provides  
35 an effective tool to assess river and marine influence: Zone I at a distance inferior to 3.0  
36 km, with  $^7\text{Be}/^{234}\text{Th}_{\text{ex}}$  inventory ratio over 0.50 (surface area near river mouth ~7 km<sup>2</sup>) is  
37 dominated by riverine particles; in contrast, Zone III at a distance superior to 8.5 km,  
38 with  $^7\text{Be}/^{234}\text{Th}_{\text{ex}}$  inventory ratio less than 0.10 (surface area off river mouth beyond 150  
39 km<sup>2</sup>) is predominantly under a marine influence. In between, an intermediate area  
40 displays a mixed influence, with inputs of riverine and marine origins: the transition Zone  
41 II at a distance between 3.0 and 8.5 km, with  $^7\text{Be}/^{234}\text{Th}_{\text{ex}}$  inventory ratios between 0.10  
42 and 0.50. This zoning could help in further understanding the spreading of  
43 particle-reactive contaminants and its initial sedimentary deposition in the Gulf of Lions.

44  
45 **Keywords:**  $^7\text{Be}$ ,  $^{234}\text{Th}$ , suspended particulate matter, Rhône River, 2008 flood, Gulf  
46 of Lions

47

48

Commenté [s1]: see the text I am not sure we need to say that if you say positively correlated

## 49 1. Introduction

50 River-dominated ocean margins are among the most biogeochemically dynamic  
51 regions of the world ocean and play a dominant role in global biogeochemical cycles  
52 (Dagg et al., 2004; McKee et al., 2004; Cai, 2011). These areas are highly efficient filters  
53 and transformers of terrestrial materials, and are key interfaces between the continent and  
54 the open ocean (Bianchi and Allison, 2009; Chen and Borges, 2009). Most of the river  
55 suspended particulate matter (SPM) is deposited in continental margin areas and less than  
56 5% reach the deep sea (McKee et al., 2004). The SPM undergoes a suite of processes  
57 associated with cycles of deposition and resuspension after its initial discharge under  
58 different hydrological conditions (Sanford, 1992), especially during river floods and  
59 ocean storms. Consequently, the study of SPM deposition in the coastal zone under  
60 different hydrological regimes, such as short-term flood events, would help in  
61 understanding the fate of terrigenous pollutants carried by the SPM in river-dominated  
62 ocean margins.

63 Natural and artificial radionuclides have been widely used to investigate various  
64 processes in estuarine, coastal and marine environments (e.g., Santschi et al., 1999;  
65 Yeager et al., 2004; Moore and Oliveira, 2008; Su et al., 2011). Generally, flood events  
66 occur over very short time-scales (from days to weeks); therefore, radionuclides with  
67 short half-lives, such as  $^7\text{Be}$  ( $t_{1/2}=53.3$  days) and  $^{234}\text{Th}$  ( $t_{1/2}=24.1$  days), appear to be  
68 appropriate tracers for studying flood deposition processes at these short time scales  
69 (Feng et al., 1999a; Saari et al., 2010). Resuspension may play a role in redistributing the  
70 original deposition and may mix sediments from different origins and age (Ogston et al.,  
71 2008).

72 Beryllium-7 ( $^7\text{Be}$ ) is produced by cosmic ray spallation of nitrogen and oxygen in  
73 the atmosphere.  $^7\text{Be}$  is a particle-reactive element and its distribution coefficient ( $K_d$ , L/kg)  
74 is estimated to be  $\sim 10^5$  in estuarine and coastal waters (Dibb and Rice, 1989; Baskaran  
75 and Swarzenski, 2007). Following its formation in the stratosphere and troposphere,  $^7\text{Be}$   
76 is scavenged by submicron aerosol particles and is delivered to land principally through  
77 precipitation and dry deposition (Lal et al., 1958; Wallbrink and Murray, 1994) and then  
78 to rivers through watershed washout (Matisoff et al., 2002).  $^7\text{Be}$  is generally used to study  
79 various processes over short time-scales, such as soil redistribution and erosion rates,

80 sediment residence time and transport in coastal and estuarine systems (Dibb and Rice,  
81 1989; Sommerfield et al., 1999; Taylor et al., 2013). Another highly particle-reactive  
82 element, Thorium-234 ( $^{234}\text{Th}$ ), with  $K_d$  up to  $\sim 10^5$ - $10^6$  (Guo et al., 1995; IAEA, 2004;  
83 Baskaran and Swarzenski, 2007), is produced from the decay of dissolved  $^{238}\text{U}$  and is  
84 commonly present in excess (ex) of its parent  $^{238}\text{U}$  in coastal suspended matter and  
85 bottom sediments (Aller and Cochran, 1976).  $^{238}\text{U}$  concentrations in rivers and oceans  
86 vary generally linearly with salinity (Skwarzec, 1995). The average  $^{238}\text{U}$  concentrations  
87 are  $41.5 \pm 2.5 \text{ Bq m}^{-3}$  ( $3.3 \pm 0.2 \mu\text{g L}^{-1}$ ) in the open ocean (salinity normalized to 35.00 ‰)  
88 and  $3.7 \pm 0.4 \text{ Bq m}^{-3}$  ( $0.3 \pm 0.03 \mu\text{g L}^{-1}$ ) in the major world rivers (Ku et al., 1977; Mangini  
89 et al., 1979; Owens et al., 2012). Therefore, the production of  $^{234}\text{Th}$  is generally greater in  
90 the seaward portion of the estuary than that in the landward part (Feng et al., 1999b).  
91 Furthermore, due to their short half-lives,  $^7\text{Be}$  and  $^{234}\text{Th}$  have proven to constitute a  
92 couple of excellent tracers to discern short-term variations in estuarine systems, such as  
93 flood deposition (Sommerfield et al., 1999; Mullenbach et al., 2004; Palinkas et al., 2005)  
94 and dynamic processes of particles and sediments (Olsen et al., 1986; Wallbrink and  
95 Murray, 1996; Feng et al., 1999a; Palinkas et al., 2005).

96 The Rhône subaqueous delta is a wave-dominated delta with micro-tidal influence  
97 and a pro-grading sedimentary structure (Syvitski and Saito, 2007), where resuspension  
98 occurs below 20 meters depth during large southeast storms occurring mostly in winter  
99 (Ulises et al., 2008; Dufois et al., 2014). Over the last two decades, numerous studies have  
100 been carried out to better understand the fate of particulate discharge from the Rhône  
101 River, especially during floods, in supplying terrigenous and river-borne material to the  
102 Mediterranean Sea and the flood impact on various processes (e.g., Milliams and Rose,  
103 2001; Perianez, 2005; Maillet et al., 2006; Miralles et al., 2006; Lansard et al., 2007;  
104 Drexler and Nittrouer, 2008; Cathalot et al., 2010; Fanget et al., 2013). They revealed that  
105 a large majority of river particles discharged into the Mediterranean Sea are deposited,  
106 biogeochemically transformed and buried close to the Rhône River mouth in the pro-delta  
107 area. The transport and deposition of the remaining SPM is mainly diverted to the  
108 southwest in the Rhône River plume. Aloisi et al. (1979) showed that SPM derived by the  
109 Rhône towards the sea is stratified in a multi-layered system (surface plume, intermediate  
110 and benthic nepheloid layers). The surface plume can spread over several kilometers off

111 the river mouth during floods (Naudin et al., 1997; Thill et al., 2001). The intermediate  
112 layers are mainly seasonal while the benthic nepheloid layer is the thickest layer, which  
113 nourishes the prodelta, shelf and slope. Therefore, defining the preferential deposition  
114 area of river-borne particles and its initial repository is of particular interest to better  
115 understand the dynamics of riverine particles and their associated contaminants drained  
116 by the Rhône River towards the Mediterranean Sea (Charmasson, 2003; Eyrolle et al.,  
117 2004; Roussiez et al., 2006, Radakovich et al., 2008).

118 The objective of our study is to define these initial particle deposition areas close to  
119 the Rhône River mouth labelled by  $^7\text{Be}$  and  $^{234}\text{Th}$  tracers, and to improve the  
120 understanding of short-term sedimentary processes in this area. It is important to  
121 document and understand the short-term deposition of riverine particles as it is strongly  
122 linked to the fate of the most labile part of the organic matter and the associated  
123 contaminants in these key regions at the land-sea interface constituted by river deltas.

124

## 125 **2. Materials and methods**

### 126 **2.1. Study area**

127 The Rhône River, one of the largest rivers in France by its freshwater discharge, has  
128 a catchment area of about 98 000 km<sup>2</sup> and 832 km length and originates from the Alps. It  
129 discharges in the Gulf of Lions (NW Mediterranean Sea) through a delta that comprises  
130 two branches, Grand Rhône (carrying 90% of the mean water discharge) and Petit Rhône  
131 (carrying the remaining 10%) (Ibanez et al., 1997). The Rhône River is the major supplier  
132 of freshwater, sediments and nutrients to the Gulf of Lions and the western Mediterranean  
133 basin (De Madron et al., 2000; Sempéré et al., 2000; Pont et al., 2002; Sadaoui et al.,  
134 2016). The mean annual river discharge was approximately 1720 m<sup>3</sup> s<sup>-1</sup> in the past sixty  
135 years. The values for the 1-year, 2-year, 10-year, 50-year, and 100-year return period (an  
136 estimate of the frequency of river flood based on a stochastic concept) of high discharge  
137 correspond to 4000, 5000, 8400, 10400 and 11200 m<sup>3</sup> s<sup>-1</sup>, respectively (Eyrolle et al.,  
138 2012 and references therein). The annual sediment discharge ranged from 0.98 to 19.7  
139 million tons (Mt, 1Mt=1×10<sup>12</sup> g), with a mean discharge of 6.7 Mt over the period  
140 1967-2008 (Pont et al., 2002; Eyrolle et al., 2012). Most of the solid load (>80%) is  
141 supplied during flood events initiated in the mountainous portions of the Rhône River

142 catchment (Pont et al., 2002; Antonelli et al., 2008). The Gulf of Lions where the Rhône  
143 discharges is micro-tidal with tidal range of 30-50 cm (Dufois et al., 2008). Therefore, the  
144 Rhône estuary is stratified and tidal mixing is insignificant. A large turbid plume of one  
145 meter in thickness (occasionally up to 5 meters) with mixed freshwater and seawater  
146 extends offshore towards the southwest (Many et al., 2018). Below this layer, the salinity  
147 of the water is the Mediterranean seawater salinity, i.e., 38 ‰. As mentioned above, large  
148 resuspension events are limited to the winter and are generally weaker during spring,  
149 summer and fall, although occasional storms may displace centimetric layers of sediment  
150 (Toussaint et al., 2014; Dufois et al., 2014). The seafloor bathymetry in the subaqueous  
151 delta shows three major domains: the proximal domain, in a radius of 2 km off the river  
152 mouth with water depth of 10-30 m; the pro-delta domain, 2-5 km off the river mouth  
153 with water depth ranging from 30 to 70 m; and the distal domain (continental shelf),  
154 beyond 5 km off the river mouth with water depth between 70 and 90 m (Got and Aloisi,  
155 1990). The subaqueous delta structure is characterized by fine-grained deposits in the  
156 proximal area below 20 meters depth (Durrieu de Madron et al., 2000; Roussiez et al.,  
157 2005). The net sedimentation rates varied from 30 to 50 cm yr<sup>-1</sup> in the proximal domain  
158 (Calmet and Fernandez, 1990; Charmasson et al., 1998), to 1-2 cm yr<sup>-1</sup> in the prodelta,  
159 down to 0.1-0.6 cm yr<sup>-1</sup> with a mean rate of 0.3 cm yr<sup>-1</sup> in the distal domain (Radakovitch  
160 et al., 1999; Miralles et al., 2005). The grain size in the entire area is quite homogeneous  
161 (D<sub>0.5</sub> =10-15µm) (Bonifacio et al., 2014; Cathalot et al., 2010). The biogeochemical  
162 characteristics are also very different between the three zones with large mineralization of  
163 organic matter involving sulfate reduction in the proximal and prodelta zones and suboxic  
164 diagenesis in the distal region (Pastor et al., 2011; Rassmann et al., 2016).

## 165 **2.2. River discharge and SPM data**

166 The Rhône River flow was provided by the CNR (*Compagnie Nationale du Rhône*)  
167 and SPM was measured at the Arles-SORA station by the MIO (*Mediterranean Institute*  
168 *of Oceanology*). Daily SPM samples were obtained by collecting automatically 150 mL  
169 of water every 90 min. Samples for SPM analysis were preserved with HgCl<sub>2</sub> and stored  
170 at 5 °C until the bulk sample volumes were filtered using 1-µm pre-conditioned glass  
171 fiber filters (ashed at 450 °C for 4 h and pre-weighed before filtration). The SPM was  
172 quantified by differential weighing after drying at 60 °C for 24 h. The analytical

173 uncertainty of SPM concentrations was  $5 \times 10^{-4}$  g L<sup>-1</sup>.

### 174 2.3. Sample collection

175 The sediment cores were collected using various corers with 20-40 cm of length  
176 that allow good preservation of the interface, i.e., Usnel box-corers, Ronanberg corer and  
177 Octopus multi-corer, during seven cruises conducted in the Gulf of Lions from March 13,  
178 2007 to December 7, 2008 (Figure 1), a period characterized by a large and unusual flood  
179 in May-June 2008 created by a dam release on the largest alpine tributary (Durance) and  
180 a more typical flood in November 2008. Before the May-June 2008 flood, 21 sediment  
181 cores were collected in March, April and September 2007, and in March 2008. Five  
182 sediment cores were sampled off the Rhône River mouth during the 2008 flood  
183 (May-June), but only one core, Stn.AK3, was sampled after the main deposition event in  
184 the pro-delta. After the 2008 flood, six stations were sampled in October and December  
185 2008. The detailed sample information is listed in Table 1. The sediment core samples  
186 were extruded onboard and sliced at depth intervals of 0.5-, 1.0- or 2.0-cm. Then, the  
187 subsamples were frozen and kept in that state until they were shipped to the shore-based  
188 laboratory, where they were dried (either at 60 °C for 24 h or freeze-dried) and pulverized  
189 using agate mortar and pestle sets.

### 190 2.4. <sup>7</sup>Be isotope measurement

191 The radionuclide measurements were carried out in two laboratories: “*Laboratoire*  
192 *Souterrain de Modane* (LSM)” in the French Alps (Reyss et al., 1995; Cazala et al., 2003)  
193 and “*Laboratoire de Mesure de la Radioactivité de l’Environnement* (LMRE)” in Orsay  
194 (IRSN) (De Vismes Ott et al., 2013). At LSM, aliquots of 3-4 g were measured in the  
195 wells of very low-background and high-efficiency germanium detectors. Protected from  
196 cosmic radiation by 1700 m of rocks, a background as low as 0.5 counts per minute from  
197 40 keV to 3000 keV was measured. Due to the short half-life, no standard for <sup>7</sup>Be was  
198 used at LSM and the efficiency-versus-energy curve was extrapolated between <sup>137</sup>Cs  
199 gamma ray at 662 keV and <sup>40</sup>K at 1460 keV to the 478 keV peak of <sup>7</sup>Be (Larsen and  
200 Cutshall, 1981). Generally, a counting time of one day for the deepest samples leads to  
201 precise data (uncertainty less than 10% for 2σ counting statistical error). At LMRE, 60  
202 mL or 220 mL (~50-300 g) sediments were measured with the coaxial or semi-planar  
203 (HPGe) germanium detectors for 24-48 hours, with a relative efficiency greater than 50%.

Commenté [s2]: if my memroy is correct with this corer we sampled cores about 60 to 80cm length, right?

Mis en forme : Anglais (États-Unis)



204 Detectors were in a room shielded with 10 cm of low-background lead and 5 mm of  
205 electrolytic copper, located underground under a 3-m-thick boron concrete slab (De  
206 Vismes Ott et al., 2013). Calibrations in energy, resolution and efficiency were carried out  
207 using standard sources (including  $^7\text{Be}$ ) prepared in the “*Laboratoire des Etalons et*  
208 *Intercomparaisons*” of the IRSN (LEI, under COFRAC accreditation), filled with an  
209 epoxide resin multi-gamma mixture source supplied by CERCA Inc (France). The  $^7\text{Be}$  was  
210 measured via its peak at 477 keV of 10.44% emission intensity. Activities of  $^7\text{Be}$  were all  
211 corrected for decay since the date of sample collection in this study, and expressed as Bq  
212  $\text{kg}^{-1}$  of dry weight of sediment. The two laboratories regularly participate in  
213 inter-comparison exercises at national and international levels and are reference  
214 laboratories in France. The results show an overall agreement between the two techniques  
215 with less than 10% difference.

## 216 2.5. $^{234}\text{Th}_{\text{ex}}$ isotope analysis

217 The dried and homogenized samples were weighed and transferred to plastic  
218 counting geometries for non-destructive analysis of  $^{234}\text{Th}$  using gamma spectrometry. At  
219 LSM, six standards were used to calibrate the gamma detectors for the determination of  
220 gamma emitters (Cazala et al., 2003).  $^{234}\text{Th}$  activity was measured in both laboratories  
221 directly from its gamma photo-peak at 63.3 keV. A correction for gamma attenuation was  
222 applied and the self-adsorption coefficient for  $^{234}\text{Th}$  was also determined according to the  
223 methods suggested by Cutshall et al. (1983), because significant self-absorption of  
224 gamma energy occurs below 295 keV. At LMRE, for this low-energy line (<100 keV), a  
225 transmission measurement was carried out to determine the attenuation coefficients of the  
226 samples in order to correct the measured activity of the self-attenuation phenomena, which  
227 may be significant for sediments, especially on large geometries (220 mL) (Lefèvre et al.,  
228 2003). In addition,  $^{234}\text{Th}$  supported by its grandparent  $^{238}\text{U}$  was determined by recounting  
229 those samples at depth in the core after approximately 5 months. The average activities  
230 measured in the second count were subtracted from the activities determined in the first  
231 counting session. This allows us to determine excess  $^{234}\text{Th}$  activities (activities not  
232 supported by  $^{238}\text{U}$ ; denoted  $^{234}\text{Th}_{\text{ex}}$ ). The counting time was at least 24 h, depending on  
233 the sample activity. The activities of the excess  $^{234}\text{Th}$  ( $^{234}\text{Th}_{\text{ex}}$ ) were all corrected for  
234 decay since the sampling date and expressed as Bq  $\text{kg}^{-1}$  of dry weight of sediment.

235 **2.6. Calculation of <sup>7</sup>Be and <sup>234</sup>Th<sub>ex</sub> inventories and SPM flux**

236 Inventories of <sup>7</sup>Be and <sup>234</sup>Th<sub>ex</sub> are useful parameters for assessing the deposition  
237 process of SPM. In this study, <sup>7</sup>Be and <sup>234</sup>Th<sub>ex</sub> inventories in dry sediments were  
238 calculated by summing their respective activities at each layer, according to the following  
239 formula (Wang and Yamada, 2005):

240 
$$I = \sum_{i=1}^N \rho_s X_i A_i \quad (1)$$

241 where  $I$  represents the inventories of <sup>7</sup>Be or <sup>234</sup>Th<sub>ex</sub> in the dry sediments (mBq cm<sup>-2</sup>),  
242  $N$  is the number of sampling layers,  $\rho_s$  is the solid phase dry density,  $X$  is the  
243 thickness of the sampling interval  $i$  (cm), and  $A$  is the activity of the sampled interval  
244 (Bq kg<sup>-1</sup>). Uncertainties on inventories are the sum of the propagated error determined for  
245 each of the sampling intervals. In some cores, <sup>7</sup>Be or <sup>234</sup>Th<sub>ex</sub> activities were still detected  
246 in the deepest sampled layers. Therefore, for these cores the activities in the un-sampled  
247 deepest layers were extrapolated by the use of an exponential equation fitted to the  
248 existing field data, to allow estimates of completed (closed) inventories.

249 The annual SPM fluxes (SPM<sub>a</sub> in kg) were calculated through the following  
250 equation (Eyrolle et al., 2012):

251 
$$SPM_a = \sum_{t=1}^{t=n} ((SPM_{ct} + SPM_{ct+1}) / 2) \cdot ((Q_t + Q_{t+1}) / 2) \cdot \Delta T \quad (2)$$

252 where  $n$  is the number of samples collected during the year,  $SPM_{ct}$  represents the SPM  
253 concentration measured over a given period of time or at the time  $t$  (mg L<sup>-1</sup>),  $Q$  is the  
254 average river flow during the sampling period (m<sup>3</sup> s<sup>-1</sup>), and  $\Delta T$  is the period of time  
255 between two continuous samples collected at times  $t$  and  $t+1$  (s). In order to take into  
256 account the fact that sediment deposition integrates several deposition events, and to  
257 better link particulate inputs and sediment inventories on the same timescale, we also  
258 calculated the cumulated SPM fluxes over two half-lives before the sampling date for  
259 each radionuclide by summing the particle discharge over this period of time, namely,  
260 ~106 d for <sup>7</sup>Be and ~48 d for <sup>234</sup>Th. For time periods longer than two half-lives before the  
261 sampling period, the radionuclide inventory will have decreased by 75% and will  
262 contribute marginally to the overall inventory.

## 263 **3. Results**

### 264 **3.1. Temporal variations of river flow rates and particulate discharge**

265 Temporal variations of river flow rates and particulate discharges measured at the  
266 SORA station located on the Grand Rhône in Arles 40 km upstream of the river mouth  
267 during the period 2007-2008 are presented in [Figure 2](#). The mean annual river flow rate  
268 over our study period is  $1566 \pm 834 \text{ m}^3 \text{ s}^{-1}$ , which is in the range of the mean value over  
269 the past sixty years ( $1720 \pm 982 \text{ m}^3 \text{ s}^{-1}$ ). At the SORA station in Arles, a river flood event is  
270 defined as a river flow rate above  $3000 \text{ m}^3 \text{ s}^{-1}$  since this threshold corresponds to a  
271 breakdown in the relationship between the river flow and SPM concentrations indicating  
272 the initiation of sediment transport under flood conditions ([Pont et al., 2002](#); [Antonelli,](#)  
273 [2002](#); [Eyrolle et al., 2012](#)). The year 2007 was defined as a “no flood” year with river  
274 flow only approaching or slightly exceeding  $3000 \text{ m}^3 \text{ s}^{-1}$  in March 4-9 and on November  
275 24 ([Figure 2a](#)) and was characterized by a very low annual particulate discharge, i.e., 1.5  
276 Mt. In contrast, the year 2008 was characterized by a succession of moderate floods with  
277 maxima of about  $4000\text{-}5000 \text{ m}^3 \text{ s}^{-1}$  ([Eyrolle et al., 2012](#); [Zebracki et al., 2015](#)). Over our  
278 2008 sampling period (ending on December 7, 2008), two main floods occurred ([Figure](#)  
279 [2b](#)): the first and main one in terms of duration started on May 28 and ended on June 12,  
280 2008 (~16 d), and the second one occurred between November 2-7, 2008 (~6 d).  
281 However, the SPM concentrations observed in May-June 2008 are exceptionally high for  
282 such a moderate flood. A mean daily SPM concentration peak reaching  $3356 \text{ mg L}^{-1}$  was  
283 recorded on June 1, 2008, with daily maximum SPM fluxes reaching  $11940 \text{ kg s}^{-1}$ . It is  
284 estimated that this atypical flood event of anthropogenic origin induced the transfer of 4.7  
285 Mt SPM towards the sea over a 16 day period, mostly from the flushing of old sediment  
286 trapped in reservoirs and the erosion of the river banks, which contains unusually low  
287 short-lived radionuclides ([Eyrolle et al., 2012](#)) and old carbon ([Cathalot et al., 2013](#)). This  
288 flood event accounts for ~52% of the 2008 annual SPM fluxes (about 9.1 Mt) and  
289 represents by itself three times the 2007 annual SPM fluxes (~1.5 Mt) ([Eyrolle et al.,](#)  
290 [2012](#)). In contrast, the SPM flux (~0.4 Mt) induced by the November flood event that  
291 reached  $4800 \text{ m}^3 \text{ s}^{-1}$  (November 2-7, 2008) only accounted for ~4% of the 2008 annual  
292 SPM flux (Grand Rhône).

### 293 **3.2. $^7\text{Be}$ activities and inventories**

294 A selection of vertical distributions of  $^7\text{Be}$  activities in the sediment cores are shown  
295 in Figure 3. Depth profiles of  $^7\text{Be}$  activities in the sediment cores showed an overall  
296 decrease with depth, which is caused by burial, bioturbation and gradual decay of  $^7\text{Be}$   
297 with depth (Fitzgerald et al., 2001; Miralles et al., 2006). The  $^7\text{Be}$  penetration depth also  
298 shows a decrease with increasing distance from the river mouth (from Stn.A to Stns. B, C,  
299 D, E and U).

300 Distributions of  $^7\text{Be}$  activities in surface sediments demonstrate spatial and temporal  
301 variations. Spatial distributions showed a clear decrease of surface  $^7\text{Be}$  activity with  
302 increasing distance from the river mouth. For example, in April 2007, along the SW  
303 direction,  $^7\text{Be}$  activities at Stn.A adjacent to the river mouth were higher than at Stns. B,  
304 N and E.

305  $^7\text{Be}$  inventories in the sediment cores are listed in Table 2 and they showed a large  
306 spatial variation with a 85-fold decrease from Stn.A in May 2008 ( $1826 \text{ mBq cm}^{-2}$ ) to  
307 Stn.U on the shelf ( $21 \text{ mBq cm}^{-2}$ ).

### 308 3.3. $^{234}\text{Th}_{\text{ex}}$ activities and inventories

309 Vertical distributions of  $^{234}\text{Th}_{\text{ex}}$  activities in sediment cores also showed a decrease  
310 with increasing depth (Figure 4). However, the horizontal distribution of surface activity  
311 is inconsistent with that of  $^7\text{Be}$ , since the  $^{234}\text{Th}_{\text{ex}}$  activities in surface sediments did not  
312 show a decrease with distance from the river mouth. Along the SW direction, the  $^{234}\text{Th}_{\text{ex}}$   
313 activity at Stn.E was higher than that of Stn.B close to the river mouth in April 2007.

314  $^{234}\text{Th}_{\text{ex}}$  inventories in the sediment cores are also listed in Table 2. They varied from  
315  $525$  to  $5474 \text{ mBq cm}^{-2}$ , showing a 10-fold decrease along the offshore transect. Within a 3  
316 km area at the river mouth,  $^{234}\text{Th}_{\text{ex}}$  inventories along the increasing distance from the  
317 river mouth varied from  $2042 \pm 668 \text{ mBq cm}^{-2}$  at Stn.A (2.1 km) to  $1294 \pm 292 \text{ mBq cm}^{-2}$  at  
318 Stn.B (2.9 km) in April 2007. During the same period,  $^{234}\text{Th}_{\text{ex}}$  inventory ( $856 \pm 89 \text{ mBq}$   
319  $\text{cm}^{-2}$ ) at Stn.E (16.6 km) appears only slightly higher compared to Stn.N ( $599 \pm 196 \text{ mBq}$   
320  $\text{cm}^{-2}$ ) closer to the coast (5.1 km). When considering their uncertainty,  $^{234}\text{Th}_{\text{ex}}$  inventories  
321 do not demonstrate a clear spatial variation as can be seen on  $^7\text{Be}$  inventory distribution.  
322 This has to be related to the differences in primary sources: a point source from the mouth  
323 for  $^7\text{Be}$ , while  $^{234}\text{Th}_{\text{ex}}$  source is more spread out since it is produced in situ from dissolved  
324 uranium in saline water.

325

## 326 **4. Discussion**

### 327 **4.1. $^7\text{Be}$ and $^{234}\text{Th}_{\text{ex}}$ as tracers of short term SPM deposition**

328 SPM concentrations in surface water decrease rapidly seaward from 20 mg L<sup>-1</sup> near  
329 the Rhône River mouth to 1.5 mg L<sup>-1</sup> at the shelf break (Many et al., 2016). Given that  
330  $^7\text{Be}$  is largely associated with riverine particles, it thus follows the main riverine SPM  
331 deposition patterns. Therefore, the clear decrease in  $^7\text{Be}$  activities with distance from the  
332 Rhône River mouth can be associated with the decreasing contribution of river-borne  
333 particles in offshore sediments.  $^7\text{Be}$  inventories also showed an exponential decrease with  
334 increasing distance from Rhône River mouth to shelf (seaward). The  $^7\text{Be}$  inventories  
335 reach low values when the distance is over 5 km (see Figure 5a) and the highest  $^7\text{Be}$   
336 inventories appear within a ~5 km radius from the Rhône River mouth due to higher  
337 activities and sediment penetration, indicating an important deposition of recent particles  
338 at these locations. The lower  $^7\text{Be}$  inventories determined in sediments beyond 5 km off  
339 the river mouth indicate lower deposition rates or deposition of aged resuspended  
340 particles. Previous observations of the diffusive oxygen fluxes into the sediment (Lansard  
341 et al., 2009; Rassmann et al., 2016), organic carbon contents and chlorophyll-a  
342 concentrations in surficial sediments (Cathalot et al., 2010; Bourgeois et al., 2011) and  
343 other organic tracers (Cathalot et al., 2013) indicated similar gradients: the labile organic  
344 matter is deposited and mineralized near the river mouth creating larger oxygen demand,  
345 and concentrations of chlorophyll-a with younger  $^{14}\text{C}$  ages of organic matter whereas  
346 shelf sediments were characterized by lower oxygen demands and older organic material.  
347 In addition, we point out the variability in the  $^7\text{Be}$  inventories obtained at Stn.A in March  
348 2007 (847 to 1915 mBq cm<sup>-2</sup>) (Table 2). This variability could be due to the fact that  
349 these cores were sampled in a channelized area characterized by high spatial variability in  
350 transport mechanisms (Maillet et al., 2006). Notwithstanding the variability at station A,  
351 the gradient between the proximal zone and the continental shelf is still very large with a  
352 50-fold decrease between the station A at lowest value and the station U. It should also be  
353 noted that our two years study did not include many winter periods where significant  
354 resuspension events occur (Ulses et al., 2008).

355 Concerning  $^{234}\text{Th}_{\text{ex}}$ , high concentrations generally indicate a marine influence as it

356 is produced by the decay of  $^{238}\text{U}$  which is enriched in seawater. However, high  $^{234}\text{Th}_{\text{ex}}$   
357 activities are also observed near the Rhône River mouth. One reason could be the large  
358 amounts of riverine particles that would enhance  $^{234}\text{Th}_{\text{ex}}$  scavenging from the saline part  
359 of the stratified water column at the river mouth (Corbett et al., 2004; McCubbin et al.,  
360 2004). Alternatively, the Rhône River could be an additional  $^{234}\text{Th}$  source, as dissolved  
361  $^{238}\text{U}$  concentrations in the Rhône River are in the range of  $7.5\text{-}20.0\text{ Bq m}^{-3}$  ( $0.6\text{-}1.6\text{ }\mu\text{g}$   
362  $\text{L}^{-1}$ ). This is 2-5 times larger than the average concentration in the world rivers ( $3.7\pm 0.4$   
363  $\text{Bq m}^{-3}$ ,  $0.3\pm 0.03\text{ }\mu\text{g L}^{-1}$ ) (Ollivier et al., 2011), but lower than the average  $^{238}\text{U}$   
364 concentration of seawater in the Mediterranean Sea, which is  $\sim 43.2\text{ Bq m}^{-3}$  ( $\sim 3.5\text{ }\mu\text{g L}^{-1}$ )  
365 (Delanghe et al., 2002). These high  $^{238}\text{U}$  concentrations in the Rhône River water could  
366 be related to the lithological composition (carbonate rocks) of the Rhône basin (Ollivier  
367 et al., 2011) and agricultural fertilizers such as phosphates containing high  $^{238}\text{U}$  used in  
368 the Rhône watershed (Eyrolle et al., 2012). Meanwhile, Zebracki et al. (2017) did not  
369 observe  $^{234}\text{Th}_{\text{ex}}$  on SPM in the Lower Rhône River at the flow rates above  $3000\text{ m}^3\text{ s}^{-1}$ .  
370 Therefore, the large  $^{238}\text{U}$  concentration encountered in the river water allows the river to  
371 be a source of  $^{234}\text{Th}$  limited to the Rhône prodelta.

372  $^{234}\text{Th}_{\text{ex}}$  inventories show a gradual decrease with increasing distance from the  
373 Rhône River mouth, and the highest  $^{234}\text{Th}_{\text{ex}}$  inventories are also observed within a  $\sim 5\text{ km}$   
374 radius off the river mouth (Figure 5b). However, high  $^{234}\text{Th}_{\text{ex}}$  inventories are still  
375 observed beyond a  $\sim 5\text{ km}$  radius off the Rhône River mouth, such as at Stns. C ( $3000$   
376  $\text{mBq cm}^{-2}$ ) and D ( $2118\text{ mBq cm}^{-2}$ ), which is different from the pattern of  $^7\text{Be}$ . Such a  
377 difference in  $^{234}\text{Th}_{\text{ex}}$  and  $^7\text{Be}$  inventory distribution can be mainly attributed to their  
378 different source terms, i.e.,  $^7\text{Be}$  source derived mainly from the river, while the  $^{234}\text{Th}_{\text{ex}}$  is  
379 linked to in situ production in saline water (Saari et al., 2010).

#### 380 4.2. Relation of $^7\text{Be}$ and $^{234}\text{Th}_{\text{ex}}$ with river particulate flux

381 Large temporal variations in  $^7\text{Be}$  activities near the river mouth (Stns. A, AB, AK)  
382 appeared to be associated with river particulate discharge. In general, high river  
383 particulate discharge corresponds to high  $^7\text{Be}$  activities in proximal zone sediments. For  
384 example, at Stn. A,  $^7\text{Be}$  activities in December 2008 were higher than that in March 2008  
385 since the river particulate discharge in December 2008 was also higher compared to

Commenté [s3]: right so it is why it is not correct to speak about marine particles idem if the Rhone is a source of  $^{234}\text{Th}$ ....

386 March 2008. Like  $^7\text{Be}$ ,  $^{234}\text{Th}_{\text{ex}}$  activities (Table 2) also seem to demonstrate a positive  
387 relation with the river particulate discharge ( $R^2=0.26$ ,  $p<0.05$ ). For example, at Stn.A,  
388  $^{234}\text{Th}_{\text{ex}}$  activities (Table 2) observed in March 2007 are higher than in September 2007  
389 when the SPM flux is lower.

390 Indeed, at this station, the periods of high  $^7\text{Be}$  and  $^{234}\text{Th}_{\text{ex}}$  inventories were associated  
391 with higher river flow and river particle discharge. Indeed, high SPM riverine fluxes in  
392 March 2007 and December 2008 led to higher  $^7\text{Be}$  and  $^{234}\text{Th}_{\text{ex}}$  inventories compared to  
393 those observed in September 2007 and March 2008 when SPM fluxes were lower.

Commenté [r4]: Agreed! This is clearer.

394 (Table 2). This agrees with a study on the western shelf of the Mississippi River  
395 delta carried out by Corbett et al. (2007), where high  $^7\text{Be}$  inventories near the Mississippi  
396 River mouth were positively related to river particulate discharge. Similar time variations  
397 of  $^7\text{Be}$  and  $^{234}\text{Th}_{\text{ex}}$  inventories were also observed in other estuarine systems, such as the  
398 Tampa Bay (Baskaran and Swarzenski, 2007), Gironde estuary (Saari et al., 2010) and  
399 Yangtze River estuary (Wang et al., 2016).

400 High inventories of short-lived radionuclides in the sediment indicate high recent  
401 deposition of particles near the river mouth and most probably preferential deposition and  
402 accumulation of sediment. Indeed, apparent accumulation rates studied in the same areas  
403 with longer half-life radionuclides such as  $^{137}\text{Cs}$  or  $^{210}\text{Pb}$  (Calmet and Fernandez, 1990;  
404 Charmasson et al., 1998; Radakocitch et al., 1999) also show large sedimentation rates  
405 near the Rhône River mouth with very high values around  $30\text{-}50\text{ cm yr}^{-1}$  and a gradual  
406 decrease with increasing distance from the shoreline. Certainly, this apparent consistency  
407 between inventories and apparent accumulation rates does not imply that once settled the  
408 bottom particles do not undergo resuspension/transport processes since this area can be  
409 very dynamic during storm events, especially during the winter (Marion et al., 2010;  
410 Dufois et al., 2014).

411 As we have seen, the activities and inventories of  $^7\text{Be}$  and  $^{234}\text{Th}_{\text{ex}}$  are only  
412 qualitatively related to river particulate discharges. This is due to the integrative timescale  
413 of sediment inventory (which spans over a few half-lives of the radionuclides) versus the  
414 instantaneous time frame captured by the daily particulate discharge. To bridge this time  
415 lag, we have integrated the SPM fluxes over the period preceding the sampling date and

416 compared it to the sediment inventory. The integration period covering two half-lives  
417 before the sampling date was chosen, i.e., 106 days for  $^7\text{Be}$  and 48 days for  $^{234}\text{Th}_{\text{ex}}$  (see in  
418 the Materials and Methods section). The cumulated SPM fluxes calculated accordingly  
419 are listed in Table 2 and compared with the  $^7\text{Be}$  inventory in sediments (Figure 7a).

420 Before discussing the correlations, it is worth noting that the SPM concentration in  
421 2008 May-June flood is similar to the December 2003 major flood ( $3669 \text{ mg L}^{-1}$  for a  
422 flow rate of about  $10000 \text{ m}^3 \text{ s}^{-1}$ ; Eyrolle et al., 2012). This atypical high particulate load is  
423 linked to the upper Durance dam management, which discharged the excess water after  
424 heavy precipitation events in the southeastern Rhône watershed (Eyrolle et al., 2012).  
425 Therefore, the Stn.AK3 (close to the river mouth and sampled after the May-June flood)  
426 is very peculiar due to the nature of the transported solid load, which was characterized as  
427 “old” material (Cathalot et al., 2013) consequently depleted in short half-life  
428 radionuclides (Eyrolle et al., 2012). Accordingly, the highest cumulated SPM flux  
429 corresponds to low short-lived radionuclide activities, resulting in lower inventories than  
430 those expected under typical flood conditions (see a broader discussion of this atypical  
431 flood in Eyrolle et al., 2012). When data from this atypical flood (Stn.AK3) were  
432 excluded,  $^7\text{Be}$  inventories show a good correlation with the cumulated SPM flux  
433 ( $R^2=0.71$ ,  $p<0.05$ ), indicating that the  $^7\text{Be}$  inventory is a fair record of the riverine  
434 particles deposition on a timescale of 3-4 months.

435 The highest  $^{234}\text{Th}_{\text{ex}}$  inventories were observed in the river mouth, such as at station  
436 A. This suggests that: 1)  $^{234}\text{Th}_{\text{ex}}$  generated by both seawater and the Rhône water was  
437 carried by particles towards the river delta (Ollivier et al., 2011); 2) the scavenging of  
438  $^{234}\text{Th}_{\text{ex}}$  was enhanced because freshwater mixing with marine water led to high turbidity  
439 and sedimentation rates (aggregation and flocculation processes) in this area. Through  
440 12-year observations (1988-2000), Corbett et al. (2004) also pointed out that the  $^{234}\text{Th}_{\text{ex}}$   
441 inventories in the Mississippi River estuary are positively correlated with river particulate  
442 discharge.  $^{234}\text{Th}_{\text{ex}}$  inventories also seem to be related to Rhône River particulate discharge  
443 although the relation with cumulated SPM fluxes over ~48 days before the sampling  
444 appears to be much weaker compared to  $^7\text{Be}$  ( $R^2=0.44$ ,  $p<0.05$ ) (Figure 7b). As  
445 mentioned above, this is likely linked to their difference in source terms, which are  
446 mainly riverine for  $^7\text{Be}$  and both riverine and marine for  $^{234}\text{Th}_{\text{ex}}$ . The  $^7\text{Be}$  and  $^{234}\text{Th}_{\text{ex}}$

Commenté [s5]: again this shows that you have riverine particles with  $^{234}\text{Th}$



447 particulate activities in the lower Rhône River ranged from 15 to 400 Bq kg<sup>-1</sup> and from  
448 unquantifiable to 56±14 Bq kg<sup>-1</sup>, respectively (Eyrolle et al., 2012; Zebracki et al., 2017).  
449 Despite the dual nature of <sup>234</sup>Th<sub>ex</sub>, the different sources allow us to define a zoning with  
450 respect to the influence of the Rhône River particulate discharge.

#### 451 **4.3. Zoning of the Rhône River influence on sediments**

452 <sup>7</sup>Be and <sup>234</sup>Th<sub>ex</sub> are both strongly bound to particulate matter, without significant  
453 difference in preferential adsorption (*K<sub>d</sub>*) at high SPM concentrations, such as in the river  
454 mouth (Baskaran et al., 1997; Baskaran and Swarzenski, 2007). The potential differences  
455 in their specific activities and inventories are mainly caused by source terms, seasonal  
456 variations of the river particulate discharge, grain size, distance of salt-water intrusion  
457 and amounts of particles in the water column (Feng et al., 1999a; Saari et al., 2010).  
458 Figure 5a clearly shows two populations of <sup>7</sup>Be inventories with large and variable values  
459 near the river mouth at stations A and AB (or AZ) which are the closest stations to the  
460 river mouth and lower values further on the shelf. It must be noted that the two possible  
461 explanations of Figure 5a (i.e. two separate inventory populations or gradual decrease  
462 offshore of the inventories) support the zoning based on <sup>7</sup>Be/<sup>234</sup>Th<sub>ex</sub> inventory. The  
463 decrease in <sup>7</sup>Be inventory offshore is persistent in time and the trend lines for 2007 and  
464 2008 show good statistics (R<sup>2</sup>=0.49 and 0.53) which lend support to a rapid decrease of  
465 <sup>7</sup>Be activity offshore. <sup>7</sup>Be is thus a powerful tracer for riverine particles although  
466 <sup>7</sup>Be-deficient sediments were exceptionally discharged by the Rhône River to the sea  
467 during the May flood event of 2008 due to rapid erosion of old watershed sediments. The  
468 situation is less clear for <sup>234</sup>Th<sub>ex</sub> as a tracer of marine influence with more variable  
469 inventory at and near the river mouth, but a decrease offshore, although much weaker  
470 than <sup>7</sup>Be, is also visible (Figure 5b). Notably, this weak decrease of <sup>234</sup>Th inventories  
471 from the mouth of the river towards the shelf in the Rhône River deltaic region is  
472 contrary to expectations if <sup>234</sup>Th is assumed to have only a marine source. The large  
473 spread observed in both radionuclides inventory is due to different source inputs, change  
474 in grain size and sediment type (Feng et al., 1999a, b). The use of <sup>7</sup>Be/<sup>234</sup>Th<sub>ex</sub> inventory  
475 ratio may allow avoiding these inventory variations and be a better indicator than <sup>7</sup>Be  
476 alone. It is noteworthy that, in other cases such as the Mississippi River deltaic region  
477 where <sup>234</sup>Th<sub>ex</sub> inventories increase with the distance off the river mouth (Corbett et al.,

478 2004), the use of  ${}^7\text{Be}/{}^{234}\text{Th}_{\text{ex}}$  inventory ratio is more powerful than the single radionuclide  
479  ${}^7\text{Be}$ .

480  
481

482 .),

483 The  ${}^7\text{Be}/{}^{234}\text{Th}_{\text{ex}}$  inventory ratios in sediment ranged from 0.02 to 0.77, with large  
484 variations with the distance from the Rhône mouth (Figure 8). The  ${}^7\text{Be}/{}^{234}\text{Th}_{\text{ex}}$  inventory  
485 ratios decreased from 0.59 at Stn.A3 (32 m water depth) to 0.04 at Stn.U (90 m water  
486 depth) in June 2008, and from 0.77 (21 m water depth) at Stn.A4 to 0.17 at Stn.C (72 m  
487 water depth) in December 2008. The lowest ratio of 0.04 indicates that the riverine source  
488 traced by  ${}^7\text{Be}$  has disappeared and that the marine influence is dominant. In contrast, the  
489 high ratio of 0.77 indicates that the riverine source is dominant. High  ${}^7\text{Be}/{}^{234}\text{Th}_{\text{ex}}$   
490 inventory ratios also mainly occur within a  $\sim 5$  km radius off the river mouth. Feng et al.  
491 (1999b) pointed out that the  ${}^7\text{Be}/{}^{234}\text{Th}_{\text{ex}}$  inventory ratios are a negative function of both  
492 the water depth and salinity in a completely different context of a partially-mixed tidal  
493 estuary, namely, increasing with the decrease of water depth and salinity. However, the  
494 Rhône River plume spreads over kilometers off the Rhône mouth and the low salinity  
495 waters are confined to a thin surface layer at the surface with seawater below the plume  
496 (Naudin et al., 1997; Amoux-Chiavassa et al., 2003; Many et al., 2016), indicating that  
497 the impact of salinity on  ${}^7\text{Be}/{}^{234}\text{Th}_{\text{ex}}$  inventory ratio can be ruled out. Thus, in our case,  
498  ${}^7\text{Be}/{}^{234}\text{Th}_{\text{ex}}$  inventory ratio is negatively correlated with water depth.

499 The  ${}^7\text{Be}/{}^{234}\text{Th}_{\text{ex}}$  inventory ratios also show temporal variations and are mainly  
500 related to river particulate discharge, especially close to the river mouth. The  ${}^7\text{Be}/{}^{234}\text{Th}_{\text{ex}}$   
501 inventory ratios during 2008 are overall higher than in 2007. The  ${}^7\text{Be}/{}^{234}\text{Th}_{\text{ex}}$  inventory  
502 ratios also demonstrated an overall positive correlation with the river particulate  
503 discharge, from normal discharge to flood discharge. At Stn.A, the  ${}^7\text{Be}/{}^{234}\text{Th}_{\text{ex}}$  inventory  
504 ratios in December 2008 (influenced by the November flood) are higher than that in  
505 March 2008, when the discharges were lower and resuspension during the end of the  
506 winter may have redistributed part of the deposited particles. In addition, as already  
507 reported, a preferential deposition towards SW is visible in our data set. In this direction  
508 at Stn.C (8.5 km away from river mouth), the  ${}^7\text{Be}/{}^{234}\text{Th}_{\text{ex}}$  inventory ratios in December

Commenté [s6]: necessary ??? not very clear, if you have a positive relationship it means that high discharge led to high inventories ratios so it is enough not need to add this..

509 2008 were three times larger than that in April 2007, showing that this station is impacted  
510 by newly deposited particles. On the contrary, in the SE direction at Stn.L (4.5 km), the  
511  ${}^7\text{Be}/{}^{234}\text{Th}_{\text{ex}}$  inventory ratio displays lower values. This feature is clearly consistent with  
512 the dominant spread direction of the Rhône River plume, generally in the SW direction,  
513 which has been proven to be the preferential direction for deposition of the riverine  
514 material in this area (Naudin et al., 1997). Similar patterns have already been reported for  
515 other tracers, such as trace metals (Alliot et al., 2003; Roussiez et al., 2006; Radakovitch  
516 et al., 2008), man-made radionuclides (Calmet and Fernandez, 1990; Charmasson, 2003;  
517 Lansard et al., 2007), and carbon and nitrogen stable isotopes (Lansard et al., 2009;  
518 Cathalot et al., 2013).

519 The use of the  ${}^7\text{Be}/{}^{234}\text{Th}_{\text{ex}}$  inventory ratio allowed us to establish a zoning  
520 regarding the particle deposition with the distance from the Rhône River mouth. In order  
521 to examine if  ${}^7\text{Be}/{}^{234}\text{Th}_{\text{ex}}$  inventory ratios have a significant difference in the different  
522 zones, we applied a simple Mann-Whitney U test (Fay and Proschan, 2010). Close to the  
523 Rhône River mouth, at a distance of less than 3.0 km, such as for Stns. A, AB and AK4,  
524 defined as Zone I (surface area near river mouth  $\sim 7 \text{ km}^2$ ),  ${}^7\text{Be}/{}^{234}\text{Th}_{\text{ex}}$  inventory ratios,  
525 ranging from 0.16 to 0.95, displays a significant difference ( $p < 0.05$ ) with the values  
526 obtained at a larger distance. These correspond to the continental shelf (distance from the  
527 river mouth  $> 8.5 \text{ km}$ ), with stations D, E, R and U designated as Zone III (surface area  
528 off river mouth  $> 150 \text{ km}^2$ ), with  ${}^7\text{Be}/{}^{234}\text{Th}_{\text{ex}}$  inventory ratios ranging from 0.02 to 0.07.  
529 This indicates that the inputs of river-borne particles are dominant in zone I, while zone  
530 III is characterized by a stronger marine particle influence. At an intermediate distance  
531 (i.e., distance from the river mouth = 3.0-8.5 km) with Stns. AZ, B, C, G, K, L, N, and O  
532 (defined as Zone II), the  ${}^7\text{Be}/{}^{234}\text{Th}_{\text{ex}}$  inventory ratios are between 0.05 and 0.30  
533 suggesting a mixed influence of particles labelled by river and seawater, recently  
534 deposited in this area. The zoning based on inventory ratios is presented in Figure 9 and  
535 summarized in Table 3. This zoning is comparable to the observation by Rassmann et al.  
536 (2016), who demonstrated that the average oxygen penetration depth into Zone I  
537 sediment was one fifth of that in Zone III. In addition, Zone I, which corresponds mainly  
538 to the pro-deltaic area, appears to be the area where most of the particle associated  
539 contaminants driven by the Rhône River into the Gulf of Lions are deposited (Miralles et

540 al., 2004; Roussiez et al., 2005). This zoning is therefore helpful for further understanding  
541 the spreading of particles-associated contaminants, such as man-made radionuclides and  
542 heavy metals, in the Gulf of Lions (Charmasson et al., 1998; Radakovitch et al., 2008;  
543 Ferrand et al., 2012) and its initial sedimentary deposition in the Gulf of Lions. This study  
544 provides an effective reference to assess riverine and marine influence beyond the Rhône,  
545 which is very important for understanding the initial deposition of riverine particles as  
546 tracking the recent particles deposition on the time scale of a few months has been rarely  
547 performed in deltas and estuaries.

548

## 549 **5. Conclusions**

550 Short-term deposition of particles close to the Rhône River mouth in the Gulf of  
551 Lions was traced by natural radionuclides  $^7\text{Be}$  and  $^{234}\text{Th}_{\text{ex}}$ . Both the  $^7\text{Be}$  and  $^{234}\text{Th}_{\text{ex}}$   
552 inventories are larger at the Rhône River mouth and were correlated with cumulated SPM  
553 fluxes calculated over two half-lives before the sampling date. The spatial distributions of  
554  $^7\text{Be}$  inventories and  $^7\text{Be}/^{234}\text{Th}_{\text{ex}}$  inventory ratios showed an exponential decrease with  
555 distance from the river mouth. Their distributions indicated that recent particles are  
556 mainly deposited within a  $\sim 5$  km radius from the river mouth and that maximal  
557 deposition occurs within 3 km off the river mouth. These areas of recently deposited  
558 particles coincide with areas with high apparent accumulation rates determined over  
559 longer time scale using longer half-life radionuclides such as  $^{137}\text{Cs}$  (ref?). Moreover, the  
560 gradients in sediment  $^7\text{Be}/^{234}\text{Th}_{\text{ex}}$  inventory ratio observed in the studied area lend  
561 support to the notion that this ratio can be used as a potential index for identifying the  
562 dominant influence between the river and the sea on the deposited particles, which is  
563 really driven by  $^7\text{Be}$  in this study. The riverine and marine influences can be classified as  
564 follows: Zone I (distance from the river mouth  $< 3.0$  km with  $^7\text{Be}/^{234}\text{Th}_{\text{ex}}$  inventory ratio  
565 over 0.50, surface area near river mouth  $\sim 7$  km<sup>2</sup>) is dominated by riverine input, while  
566 Zone III (distance from the river mouth beyond 8.5 km with  $^7\text{Be}/^{234}\text{Th}_{\text{ex}}$  inventory ratio  
567 less than 0.10, surface area off river mouth beyond 150 km<sup>2</sup>) is predominantly under a  
568 marine influence. In between, the transition zone displays a mixed influence, (transition  
569 Zone II, distance from the river mouth: 3.0-8.5 km with  $^7\text{Be}/^{234}\text{Th}_{\text{ex}}$  inventory ratios  
570 between 0.10 and 0.50).

Commenté [s7]: no need to repeat

571

572

### 573 **Author information**

#### 574 \* **Corresponding authors:**

575 Tel: +33-4-94-30-48-29, Fax: +33-4-94-30-44-16 (S. Charmasson).

576 E-mail: [christophe.rabouille@lsce.ipsl.fr](mailto:christophe.rabouille@lsce.ipsl.fr) (C. Rabouille).

577 [sabine.charmasson@irsn.fr](mailto:sabine.charmasson@irsn.fr) (S. Charmasson).

Code de champ modifié

Code de champ modifié

#### 578 **Notes**

579 The authors declare that there is no competing financial interest.

#### 580 **Author Contributions**

581 The manuscript was written through contributions from all authors. All authors have  
582 given approval to the final version of the manuscript.

583

#### 584 **Acknowledgements**

585 This work was supported by the AMORAD project (French state financial support  
586 managed by the National Agency for Research allocated in the “Investments for the  
587 Future” framework program under reference ANR-11-RSNR-0002), and funding project  
588 for scientific research startup of Shantou University. Funding was also provided by the  
589 Midi Pyrénées-Paca Interregional Project CARMA, ANR-EXTREMA, ANR-CHACCRA  
590 the EC2CO Riomar.fr, and Mistrals/Mermex through the “Mermex-Rivers” action. We  
591 thank the captains and crews of the R.V. Europe and Tethys II for their collaboration  
592 during the sampling expeditions. We deeply thank Mireille Arnaud, chief scientist of the  
593 CARMEX (March 2007) and Extrema1 (March 2008) cruises. We are very grateful to  
594 *Compagnie Nationale du Rhône* and *MOOSE/SORA observatory* in Arles for providing  
595 freshwater discharge and particle load data, respectively.

596

#### 597 **References**

598 Aller, R.C., Cochran, J.K., 1976.  $^{234}\text{Th}/^{238}\text{U}$  disequilibrium in near-shore sediment:  
599 particle reworking and diagenetic time scales. *Earth Planet. Sci. Lett.* 29, 37-50.

600 Alliot, E., Younes, W.A., Romano, J.C., Rebouillon, P., Masse, H., 2003. Biogeochemical

601 impact of a dilution plume (Rhône River) on coastal sediments: comparison between a  
602 surface water survey (1996-2000) and sediment composition. *Estuar. Coast. Shelf Sci.*  
603 *57*, 357-367.

604 Aloisi, J.C., Millot, C., Monaco, A., Pauc, H., 1979. Dynamique des suspensions et  
605 mecanismes sedimentologiques sur le plateau continental du Golfe du Lion. *C.R. Acad.*  
606 *Sci. Paris D 289*, 879-882.

607 Antonelli, C., 2002. Flux sedimentaires et morphogenese recente dans le chenal du Rhône  
608 aval. Universite de Provence, Aix en Provence, pp 272.

609 Antonelli, C., Eyrolle, F., Rolland, B., Provansal, M., Sabatier, F., 2008. Suspended  
610 sediment and  $^{137}\text{Cs}$  fluxes during the exceptional December 2003 flood in the Rhône  
611 River, southeast France. *Geomorphology 95*, 350-360.

612 Arnoux-Chiavassa, S., Rey, V., Fraunie, P., 2003. Modeling 3D Rhône River plume using  
613 a higher order advection scheme. *Oceanol. Acta 26*, 299-309.

614 Baskaran, M., Ravichandran, M., Bianchi, T.S., 1997. Cycling of  $^7\text{Be}$  and  $^{210}\text{Pb}$  in a high  
615 DOC shallow, turbid estuary of south-east Texas. *Estuar. Coast. Shelf Sci. 45*, 165-176.

616 Baskaran, M., Swarzenski, P.W., 2007. Seasonal variations on the residence times and  
617 partitioning of short-lived radionuclides ( $^{234}\text{Th}$ ,  $^7\text{Be}$  and  $^{210}\text{Pb}$ ) and depositional fluxes  
618 of  $^7\text{Be}$  and  $^{210}\text{Pb}$  in Tampa Bay, Florida. *Mar. Chem. 104*, 27-42.

619 Bianchi, T.S., Allison, M.A., 2009. Large-river delta-front estuaries as natural “recorders”  
620 of global environmental change. *Proc. Nat. Acad. Sci. 106*, 8085-8092.

621 Bonifacio, P., Bourgeois, S., Labrune, C., Amourous, J.M., Escoubeyrou, K., Buscail, R.,  
622 Romero-Ramirez, A., Lantoine, F., Vetion, G., Bichon, S., Desmalades, M., Riviere, B.,  
623 Deflandre, B., Gremare, A., 2014. Spatiotemporal changes in surface sediment  
624 characteristics and benthic macrofauna composition off the Rhône River in relation to  
625 its hydrological regime. *Estuar. Coast. Shelf Sci. 151*, 196-209.

626 Bourgeois, S., Pruski, A.M., Sun, M. Y., Buscail, R., Lantoine, F., Kerherve, P., Vetion, G.,  
627 Riviere, B., Charles, F., 2011. Distribution and lability of land-derived organic matter  
628 in the surface sediments of the Rhône prodelta and the adjacent shelf (Mediterranean  
629 Sea, France): a multi proxy study. *Biogeosciences 8*, 3107-3125.

630 Cai, W.J., 2011. Estuarine and coastal ocean carbon paradox:  $\text{CO}_2$  sinks or sites of  
631 terrestrial carbon incineration. *Ann. Rev. Mar. Sci. 3*, 123-145.

632 Calmet, D., Fernandez, J.M., 1990. Caesium distribution in northwest Mediterranean  
633 seawater, suspended particles and sediments. *Cont. Shelf Res.* 10, 895-913.

634 Cathalot, C., Rabouille, C., Pastor, L., Deflandre, B., Viollier, E., Buscail, R., Gremare, A.,  
635 Treignier, C., Pruski, A., 2010. Temporal variability of carbon recycling in coastal  
636 sediments influenced by rivers: assessing the impact of flood inputs in the Rhône River  
637 prodelta. *Biogeosciences* 7, 1187-1205.

638 Cathalot, C., Rabouille, C., Tisnerat-Laborde, N., Toussaint, F., Kerherve, P., Buscail, R.,  
639 Loftis, K., Sun, M.Y., Tronczynski, J., Azoury, S., Lansard, B., Treignier, C., Pastor, L.,  
640 Tesi, T., 2013. The fate of river organic carbon in coastal areas: a study in the Rhône  
641 River delta using multiple isotopic ( $\delta^{13}\text{C}$ ,  $\Delta^{14}\text{C}$ ) and organic tracers. *Geochim.*  
642 *Cosmochim. Acta* 118, 33-55.

643 Cazala, C., Reyss, J.L., Decossas, J.L., Royer, A., 2003. Improvement in the  
644 determination of  $^{238}\text{U}$ ,  $^{228-234}\text{Th}$ ,  $^{226-228}\text{Ra}$ ,  $^{210}\text{Pb}$  and  $^7\text{Be}$  by spectrometry on evaporated  
645 fresh water samples. *Environ.Sci. Technol.* 37, 4990-4993.

646 Charmasson, S., 2003.  $^{137}\text{Cs}$  inventory in sediment near the Rhône mouth: role played by  
647 different sources. *Oceanol. Acta* 26, 435-441.

648 Charmasson, S., Bouisset, P., Radakovitch, O., Pruchon, A.S., Amaud, M., 1998.  
649 Long-core profiles of  $^{137}\text{Cs}$ ,  $^{134}\text{Cs}$ ,  $^{60}\text{Co}$  and  $^{210}\text{Pb}$  in sediment near the Rhône River  
650 (Northwestern Mediterranean Sea). *Estuaries* 21, 367-378.

651 Chen, C.T.A., Borges, A.V., 2009. Continental shelves as sinks and near-shore  
652 ecosystems as sources of atmospheric  $\text{CO}_2$ . *Deep-Sea Res.* 56, 578-590.

653 Corbett, D.R., Dail, M., McKee, B., 2007. High-frequency time-series of the dynamic  
654 sedimentation processes on the western shelf of the Mississippi River deltaic. *Cont.*  
655 *Shelf Res.* 27, 1600-1615.

656 Corbett, D.R., McKee, B., Duncan, D., 2004. An evaluation of mobile mud dynamics in  
657 the Mississippi River deltaic region. *Mar. Geol.* 209, 91-112.

658 Cutshall, N.H., Larsen, I.L., Olsen, C.R., 1983. Direct analysis of  $^{210}\text{Pb}$  in sediment  
659 samples: self-adsorption corrections. *Nucl. Instrum. Methods* 206, 309-312.

660 Dagg, M., Benner, R., Lohrenz, S., Lawrence, D., 2004. Transformation of dissolved and  
661 particulate materials on continental shelves influenced by large rivers: plume processes.  
662 *Cont. Shelf Res.* 24, 833-858.

663 De Madron, X.D., Abassi, A., Heussner, S., Monaco, A., Aloisi, J.C., Radakovitch, O.,  
664 Giresse, P., Buscail, R., Kerherve, P., 2000. Particulate matter and organic carbon  
665 budgets for the Gulf of Lions (NW Mediterranean). *Oceanol. Acta* 23, 717-730.  
666 De Vismes Ott, A., Gurriaran, R., Cagnat, X., Masson, O., 2013. Fission product activity  
667 ratios measured at trace level over France during the Fukushima accident. *J. Environ.*  
668 *Radioact.* 125, 6-16.  
669 Delanghe, D., Bard, E., Hamelin, B., 2002. New TIMS constraints on the uranium-238  
670 and uranium-234 in seawaters from the main ocean basins and the Mediterranean Sea.  
671 *Mar. Chem.* 80, 79-93.  
672 Dobb, J.E., Rice, D.L., 1989. The geochemistry of beryllium-7 in Chesapeake Bay. *Estuar.*  
673 *Coast. Shelf Sci.* 28, 379-394.  
674 Drexler, T.M., Nittrouer, C.A., 2008. Stratigraphic signatures due to flood deposition near  
675 the Rhône River: Gulf of Lions, northwest Mediterranean Sea. *Cont. Shelf Res.* 28,  
676 1877-1894.  
677 Dufois, F., Garreau, P., Le Hir, P., Forget, P., 2008. Wave- and current-induced bottom  
678 shear stress distribution in the Gulf of Lions. *Cont. Shelf Res.* 28, 1920-1934.  
679 Dufois, F., Verney, R., Le Hir, P., Dumas, F., Charmasson, S., 2014. Impact of winter  
680 storms on sediment erosion in the Rhône River prodelta and fate of sediment in the  
681 Gulf of Lions (North Western Mediterranean Sea). *Cont. Shelf Res.* 72, 57-72.  
682 Durrieu de Madron, X., Abassi, A., Heussner, S., Monaco, A., Aloisi, J.C., Radakovitch,  
683 O., Giresse, P., Buscail, R., Kerherve, P., 2000. Particulate matter and organic carbon  
684 budgets for the Gulf of Lions (NW Mediterranean). *Oceanol. Acta* 23, 717-730.  
685 Eyrolle, F., Charmasson, S., Louvat, D., 2004. Plutonium isotopes in the lower reaches of  
686 the river Rhône over the period 1945-2000: fluxes towards the Mediterranean Sea and  
687 sedimentary inventories. *J. Environ. Radioact.* 74, 127-138.  
688 Eyrolle, F., Radakovitch, O., Raimbault, P., Charmasson, S., Antonelli, C., Ferrand, E.,  
689 Aubert, D., Raccasi, G., Jacquet, S., Gurriaran, R., 2012. Consequences of  
690 hydrological events on the delivery of suspended sediment and associated  
691 radionuclides from the Rhône River to the Mediterranean Sea. *J. Soils Sediment* 12,  
692 1479-1495.  
693 Fanget, A.S., Bassetti, M.A., Arnaud, M., Chiffolleau, J.F., Cossa, D., Goineau, A.,



694 Fontanier, C., Buscail, R., Jouet, G., Maillet, G. M., Negri, A., Dennielou, B., Berne, S.,  
695 2013. Historical evolution and extreme climate events during the last 400 years on the  
696 Rhône prodelta (NW Mediterranean). *Mar. Geol.* 346, 375-391.

697 Fay, M.P., Proschan, M.A., 2010. Wilcoxon-Mann-Whitney or t-test? On assumptions for  
698 hypothesis tests and multiple interpretations of decision rules. *Stat. Surv.* 4, 1-39.

699 Feng, H., Cochran, J. K., Hirschberg, D.J., 1999a.  $^{234}\text{Th}$  and  $^7\text{Be}$  as tracers for transport  
700 and dynamics of suspended particles in a partially mixed estuary. *Geochim.*  
701 *Cosmochim. Acta* 63, 2487-2505.

702 Feng, H., Cochran, J.K., Hirschberg, D.J., 1999b.  $^{234}\text{Th}$  and  $^7\text{Be}$  as tracers for transport  
703 and sources of particle-associated contaminants in the Hudson River Estuary. *Sci. Total*  
704 *Environ.* 237/238, 401-418.

705 Ferrand, E., Eyrolle, F., Radakovitch, O., Provansal, M., Dufour, S., Vella, C., Raccasi, G.,  
706 Gurriaran, R., 2012. Historical levels of heavy metals and artificial radionuclides  
707 reconstructed from overbank sediment records in lower Rhône River (South-East  
708 France). *Geochim. Cosmochim. Acta* 82, 163-182.

709 Fitzgerald, S.A., Klump, J.V., Swarzenski, P.W., Mackenzie, R.A., Richards, K.D., 2001.  
710 Beryllium-7 as a tracer of short-term sediment deposition and resuspension in the Fox  
711 River, Wisconsin. *Environ. Sci. Technol.* 35, 300-305.

712 Got, H., Aloisi, J.C., 1990. The Holocene sedimentation on the Gulf of Lions margin: a  
713 quantitative approach. *Cont. Shelf Res.* 10, 841-855.

714 Guo, L.D., Santschi, P.H., Baskaran, H., Zindler, A., 1995. Distribution of dissolved and  
715 particulate  $^{230}\text{Th}$  and  $^{232}\text{Th}$  in seawater from the Gulf of Mexico and off Cape Hatteras  
716 as measured by SIMS. *Earth Planet. Sci. Lett.* 133, 117-128.

717 IAEA, 2004. Sediment distribution coefficients and concentration factors for biota in the  
718 marine environment. Technical Reports Series 422, IAEA, Vienna, pp 95.

719 Ibanez, C., Pont, D., Prat, N., 1997. Characterization of the Ebre and Rhône estuaries: a  
720 basis for defining and classifying salt-wedge estuaries. *Limnol. Oceanogr.* 42, 89-101.

721 Ku, T.L., Knauss, K.G., Mathieu, G.G., 1977. Uranium in open ocean: concentration and  
722 isotopic composition. *Deep-Sea Res.* 24, 1005-1017.

723 Lal, D., Malhotra, P.K., Peters, B., 1958. On the production of radioisotopes in the  
724 atmosphere by cosmic radiation and their application to meteorology. *J. Atoms. Terr.*

725 Phys. 12, 306-328.

726 Lansard, B., Charmasson, S., Gasco, C., Anton, M.P., Grenz, C., Arnaud, M., 2007.

727 Spatial and temporal variations of plutonium isotopes ( $^{238}\text{Pu}$  and  $^{239,240}\text{Pu}$ ) in sediments

728 off the Rhône River mouth (NW Mediterranean). *Sci. Total Environ.* 376, 215-227.

729 Lansard, B., Rabouille, C., Denis, L., Grenz, C., 2009. Benthic remineralization at the

730 land-ocean interface: a case study of the Rhône River (NW Mediterranean Sea). *Estuar.*

731 *Coast. Shelf Sci.* 81, 544-554.

732 Larsen, I.L., Cutshall, N.H., 1981. Direct determination of  $^7\text{Be}$  in sediments. *Earth Planet.*

733 *Sci. Lett.* 54, 379-384.

734 Lefevre, O., Bouisset, P., Germain, P., Barker, E., Kerlau, G., Cagnat, X., 2003.

735 Self-absorption correction factor applied to  $^{129}\text{I}$  measurement by direct gamma-X

736 spectrometry for *Fucus serratus* samples. *Nucl. Instr. Meth. Phys. Res. A* 506, 173-185.

737 Maillet, G.M., Vella, C., Berne, S., Friend, P.L., Amos, C.L., Fleury, T.J., Normand, A.,

738 2006. Morphological changes and sedimentary processes induced by the December

739 2003 flood event at the present mouth of the Grand Rhône River (southern France).

740 *Mar. Geol.* 234, 159-177.

741 Mangini, A., Sonntag, C., Bertsch, G., Muller, E., 1979. Evidence for a high natural

742 uranium content in world rivers. *Nature* 278, 337-339.

743 Many, G., Bourrin, F., Durrieu de Madron, X., Pairaud, I., Gangloff, A., Doxaran, D., Ody,

744 A., Verney, R., Menniti, C., Le Berre, D., Jacquet, M., 2016. Particle assemblage

745 characterization in the Rhône River ROFI. *J. Mar. Syst.* 157, 39-51.

746 Many, G., Bourrin, F., Durrieu de Madron, X., Ody, A., Doxaran, D., 2018. Glider and

747 satellite monitoring of the variability of the suspended particle distribution and size in

748 the Rhône ROFI. *Progr. Oceanogr.* 163, 123-135.

749 Marion, C., Dufois, F., Arnaud, M., Vella, C., 2010. In situ record of sedimentary

750 processes near the Rhône River mouth during winter events (Gulf of Lions,

751 Mediterranean Sea). *Cont. Shelf Res.* 30, 1095-1107.

752 Matisoff, G., Bonniwell, E.C., Whiting, P.J., 2002. Soil erosion and sediment sources in

753 an Ohio watershed using beryllium-7, cesium-137, and lead-210. *J. Environ. Qual.* 31,

754 54-61.

755 McCubbin, D., Leonard, K.S., Greenwood, R.C., Taylor, B.R., 2004. Solid-solution

756 partitioning of plutonium in surface waters at the Atomic Weapons Establishment  
757 Aldermaston (UK). *Sci. Total Environ.* 332, 203-216.

758 McKee, B.A., Aller, R.C., Allison, M.A., Bianchi, T.S., Kineke, G.C., 2004. Transport  
759 and transformation of dissolved and particulate materials on continental margins  
760 influenced by major rivers: benthic boundary layer and seabed processes. *Cont. Shelf*  
761 *Res.* 24, 899-926.

762 Milliams, J., Rose, C.P., 2001. Measured and predicted rates of sediment transport in  
763 storm conditions. *Mar. Geol.* 179, 121-133.

764 Miralles, J., Arnaud, M., Radakovitch, O., Marion, C., Cagnat, X., 2006. Radionuclide  
765 deposition in the Rhône River Prodelta (NW Mediterranean Sea) in response to the  
766 December 2003 extreme flood. *Mar. Geol.* 234, 179-189.

767 Miralles, J., Radakovitch, O., Aloisi, J.C., 2005.  $^{210}\text{Pb}$  sedimentation rates from the  
768 Northwestern Mediterranean margin. *Mar. Geol.* 216, 155-167.

769 Miralles, J., Radakovitch, O., Cochran, J.K., Veron, A., Masque, P., 2004. Multitracer  
770 study of anthropogenic contamination records in the Camargue, Southern France. *Sci.*  
771 *Total Environ.* 320, 63-72.

772 Moore, W.S., de Oliveira, J., 2008. Determination of residence time and mixing processes  
773 of the Ubatuba, Brazil, inner shelf waters using natural Ra isotopes. *Estuar. Coast.*  
774 *Shelf Sci.* 76, 512-521.

775 Mullenbach, B.L., Nittrouer, C.A., Puig, P., Orange, D.L., 2004. Sediment deposition in a  
776 modern submarine canyon: Eel Canyon, Northern California. *Mar. Geol.* 211, 101-119.

777 Naudin, J.J., Cauwet, G., Chretiennot-Dinet, M.J., Deniaux, B., Devenon, J.L., Pauc, H.,  
778 1997. River discharge and wind influence upon particulate transfer at the land-ocean  
779 interaction: case study of the Rhône River plume. *Estuar. Coast. Shelf Sci.* 45,  
780 303-316.

781 Ogston, A.S., Drexler, T.M., Puig, P., 2008. Sediment delivery, resuspension, and  
782 transport in two contrasting canyon environments in the southwest Gulf of Lions. *Cont.*  
783 *Shelf Res.* 28, 2000-2016.

784 Ollivier, P., Radakovitch, O., Hamelin, B., 2011. Major and trace element partition and  
785 fluxes in the Rhône River. *Chem. Geol.* 285, 15-31.

786 Olsen, C.R., Larsen, I.L., Lowry, P.D., Cutshall, N.H., Nichols, M.M., 1986.

787 Geochemistry and deposition of  $^7\text{Be}$  in river-estuarine and coastal water. *J. Geophys.*  
788 *Res.* 91, 896-908.

789 Owens, S.A., Buesseler, K.O., Sims, K.W.W., 2012. Re-evaluating the  $^{238}\text{U}$ -salinity  
790 relationship in seawater: implications for the  $^{238}\text{U}$ - $^{234}\text{Th}$  disequilibrium method. *Mar.*  
791 *Chem.* 127, 31-39.

792 Palinkas, C.M., Nittrouer, C.A., Wheatcroft, R.A., Langone, L., 2005. The use of  $^7\text{Be}$  to  
793 identify event and seasonal sedimentation near the Po River delta, Adriatic Sea. *Mar.*  
794 *Geol.* 222/223, 95-112.

795 Pastor, L., Deflandre, B., Viollier, E., Cathalot, C., Metzger, E., Rabouille, C.,  
796 Escoubeyrou, K., Lloret, E., Pruski, A.M., Vétion, G., Desmalades, M., Buscail, R.,  
797 Gremare, A., 2011. Influence of the organic matter composition on benthic oxygen  
798 demand in the Rhône River prodelta (NW Mediterranean Sea). *Cont. Shelf Res.* 31,  
799 1008-1019.

800 Perianez, R., 2005. Modelling the transport of suspended particulate matter by the Rhône  
801 River plume (France). Implications for pollutant dispersion. *Environ. Pollut.* 133,  
802 351-364.

803 Pont, D., Simonnet, J.P., Walter, A.V., 2002. Medium-term changes in suspended  
804 sediment delivery to the ocean: consequences of catchment heterogeneity and river  
805 management (Rhône River, France). *Estuar. Coast. Shelf Sci.* 54, 1-18.

806 Radakovitch, O., Charmasson, S., Arnaud, M., Bouisset, P., 1999.  $^{210}\text{Pb}$  and caesium  
807 accumulation in the Rhône delta sediment. *Estuar. Coast. Shelf Sci.* 48, 77-99.

808 Radakovitch, O., Roussiez, V., Ollivier, P., Ludwig, W., Grenz, C., Probst, J.L., 2008.  
809 Input of particulate heavy metals from rivers and associated sedimentary deposits on  
810 the Gulf of Lion continental shelf. *Estuar. Coast. Shelf Sci.* 77, 285-295.

811 Rassmann, J., Lansard, B., Pozzato, L., Rabouille, C., 2016. Carbonate chemistry in  
812 sediment porewaters of the Rhône River delta driven by early diagenesis (northwestern  
813 Mediterranean). *Biogeosciences* 13, 5379-5394.

814 Reyss, J.L., Schmidt, S., Legeleux, F., Bonté, P., 1995. Large, low background well type  
815 detectors for the measurement of environmental radioactivity. *Nucl. Instrum. Methods*  
816 *Physic. Res. Sec A* 357, 391-397.

817 Roussiez, V., Aloisi, J.C., Monaco, A., Ludwig, W., 2005. Early muddy deposits along the

818 Gulf of Lions shoreline: A key for a better understanding of land-to-sea transfer of  
819 sediments and associated pollutant fluxes. *Mar. Geol.* 222-223, 345-358.

820 Roussiez, V., Ludwig, W., Monaco, A., Probst, J.L., Bouloubassi, I., Buscaïl, R., Saragoni,  
821 G., 2006. Sources and sinks of sediment-bound contaminants in the Gulf of Lions (NW  
822 Mediterranean Sea): a multi-tracer approach. *Cont. Shelf Res.* 26, 1843-1857.

823 Saari, H.K., Schmidt, S., Castaing, P., Blanc, G., Sautour, B., Masson, O., Cochran, J.K.,  
824 2010. The particulate  ${}^7\text{Be}/{}^{210}\text{Pb}_{\text{xs}}$  and  ${}^{234}\text{Th}/{}^{210}\text{Pb}_{\text{xs}}$  activity ratios as tracers for  
825 tidal-to-seasonal particle dynamics in the Gironde estuary (France): Implications for  
826 the budget of particle-associated contaminants. *Sci. Total Environ.* 408, 4784-4794.

827 Sadaoui, M., Ludwig, W., Bourrin, F., Raimbault, P., 2016. Controls, budgets and  
828 variability of riverine sediment fluxes to the Gulf of Lions (NW Mediterranean Sea). *J.*  
829 *Hydrol.* 540, 1002-1015.

830 Sanford, L.P., 1992. New sedimentation, resuspension, and burial. *Limnol. Oceanogr.* 37,  
831 1164-1178.

832 Santschi, P.H., Guo, L., Walsh, I.D., Quigley, M.S., Baskaran, M., 1999. Boundary  
833 exchange and scavenging of radionuclides in continental margin waters of the Middle  
834 Atlantic Bight: implications for organic carbon fluxes. *Cont. Shelf Res.* 19, 609-636.

835 Sempéré, R., Charriere, B., Van Wambeke, F., Cauwet, G., 2000. Carbon inputs of the  
836 Rhône River to the Mediterranean Sea: biogeochemical implications. *Glob.*  
837 *Biogeochem. Cy.* 14, 669-681.

838 Skwarzec, B., 1995. Polonium, uranium and plutonium in southern Baltic ecosystem.  
839 Thesis and monographies, Institute of Oceanology PAN, 6, Sopot.

840 Sommerfield, C.K., Nittrouer, C.A., Alexander, C.R., 1999.  ${}^7\text{Be}$  as a tracer of flood  
841 sedimentation on the northern California continental margin. *Cont. Shelf Res.* 19,  
842 335-361.

843 Su, N., Du, J., Moore, W.S., Liu, S., Zhang, J., 2011. An examination of groundwater  
844 discharge and the associated nutrient fluxes into the estuaries of eastern Hainan Island,  
845 China using  ${}^{226}\text{Ra}$ . *Sci. Total Environ.* 409, 3909-3918.

846 Syvitski, J.P.M., Saito, Y., 2007. Morphodynamics of deltas under the influence of  
847 humans. *Glob. Planet. Change* 57, 261-282.

848 Taylor, A., Blake, W.H., Smith, H.G., Mabit, L., Keith-Roach, M.J., 2013. Assumptions

849 and challenges in the use of fallout beryllium-7 as a soil and sediment tracer in river  
850 basins. *Earth Sci. Rev.* 126, 85-95.

851 Thill, A., Moustier, S., Garnier, J.M., Estournel, C., Naudin, J.J., Bottero, J.Y., 2001.  
852 Evolution of particle size and concentration in the Rhône River mixing zone: influence  
853 of salt flocculation. *Cont. Shelf Res.* 21, 2127-2140.

854 Ulses, C., Estournel, C., Durrieu de Madron, X., Palanques, A., 2008. Suspended  
855 sediment transport in the Gulf of Lions (NW Mediterranean): impact of extreme storms  
856 and floods. *Cont. Shelf Res.* 28, 2048-2070.

857 Wallbrink, P.J., Murray, A.S., 1994. Fallout of  $^7\text{Be}$  in south Eastern Australia. *J. Environ.*  
858 *Radioact.* 25, 213-228.

859 Wallbrink, P.J., Murray, A.S., 1996. Distribution and variability of  $^7\text{Be}$  in soils under  
860 different surface cover conditions and its potential for describing soil redistribution  
861 processes. *Water Resour. Res.* 32, 467-476.

862 Wang, J.L., Du, J.Z., Baskaran, M., Zhang, J., 2016. Mobile mud dynamics in the East  
863 China Sea elucidated using  $^{210}\text{Pb}$ ,  $^{137}\text{Cs}$ ,  $^7\text{Be}$ , and  $^{234}\text{Th}$  as tracers. *J. Geophys. Res.*  
864 *Oceans* 121, 224-239.

865 Wang, Z.L., Yamada, M., 2005. Plutonium activities and  $^{240}\text{Pu}/^{239}\text{Pu}$  atom ratios in  
866 sediment cores from the East China Sea and Okinawa Trough: sources and inventories.  
867 *Earth Planet. Sci. Lett.* 233, 441-453.

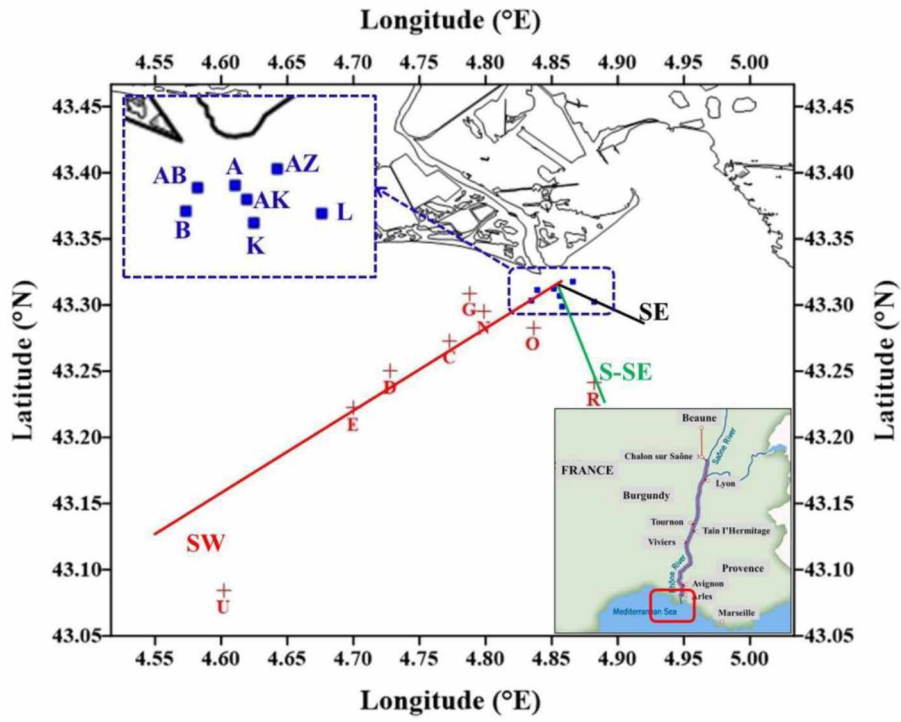
868 Yeager, K.M., Santschi, P.H., Rowe, G.T., 2004. Sediment accumulation and radionuclide  
869 inventories (Pu-239, Pu-240, Pu-210 and Th-234) in the northern Gulf of Mexico, as  
870 influenced by organic matter and macrofaunal density. *Mar. Chem.* 91, 1-14.

871 Zebracki, M., Cagnat, X., Gairoard, S., Cariou, N., Eyrolle, F., Boulet, B., Antonelli, C.,  
872 2017. U isotopes distribution in the lower Rhône River and its implication on  
873 radionuclides disequilibrium within the decay series. *J. Environ. Radioact.* 178-179,  
874 279-289.

875 Zebracki, M., Eyrolle, F., Evrard, O., Claval, D., Mourier, B., Gairoard, S., Cagnat, X.,  
876 Antonelli, C., 2015. Tracing the origin of suspended sediment in a large Mediterranean  
877 river by combining continuous river monitoring and measurement of artificial and  
878 natural radionuclides. *Sci. Total Environ.* 502, 122-132.

879

880



881

882 **Figure 1.** Maps of the Rhône River pro-delta showing the sampling locations.

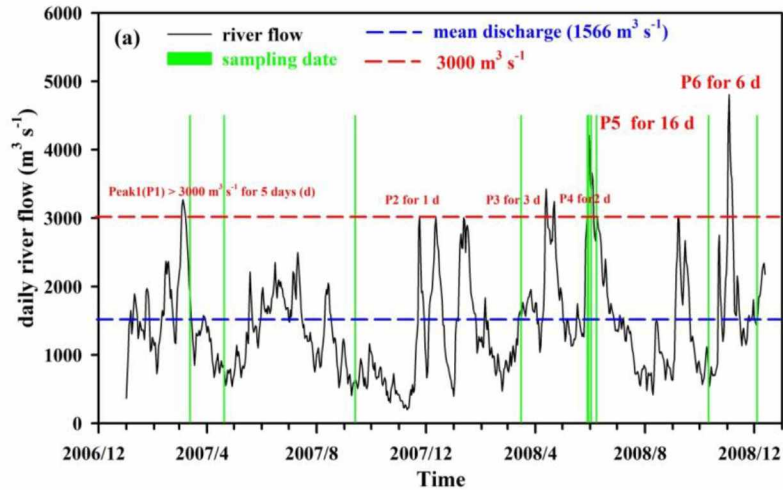
883

884

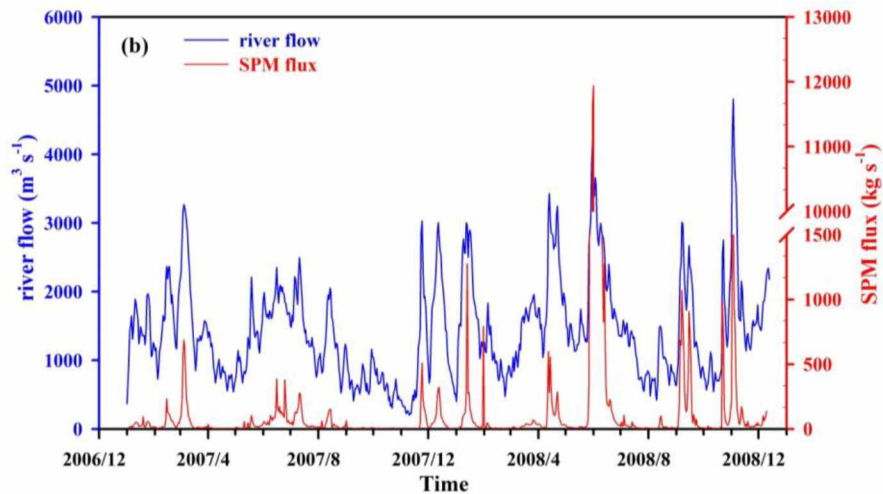
885

886

887



888



889

890 **Figure 2.** The daily variation of the Rhône River flow (a) and the relationship between  
 891 river flow and Suspended Particulate Matter (SPM) fluxes (b) during the period of  
 892 2007-2008.

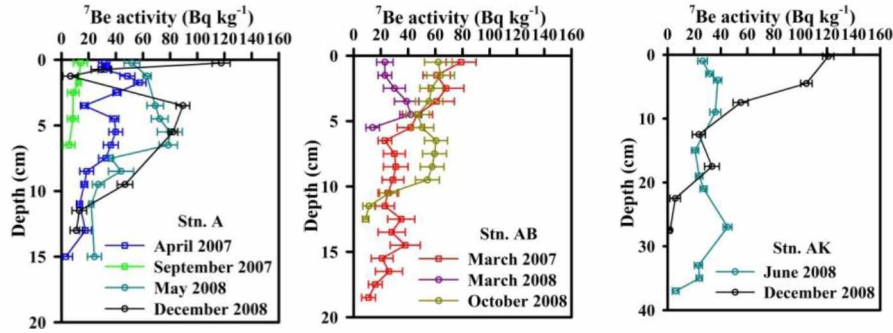
893

894

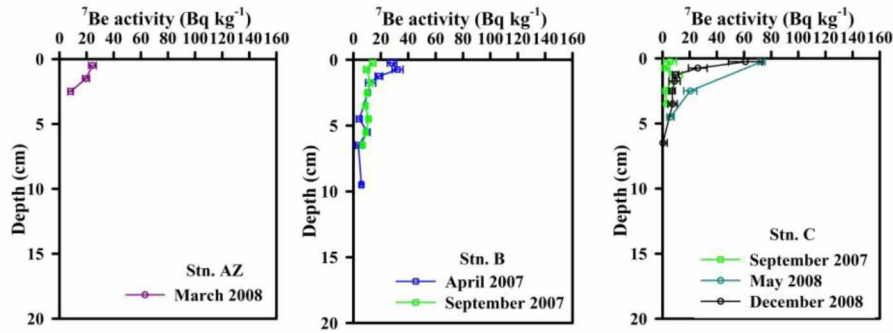
895



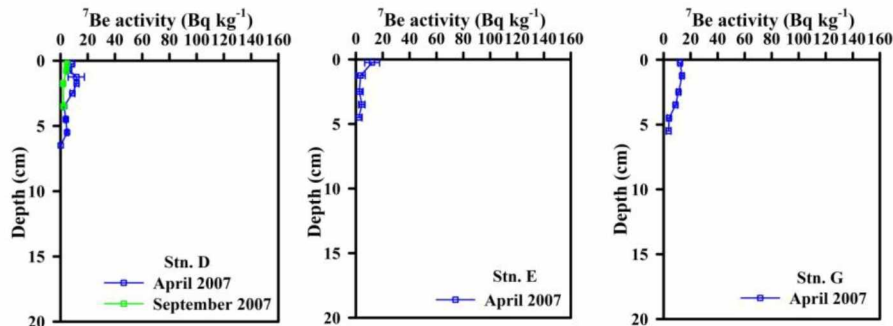
896

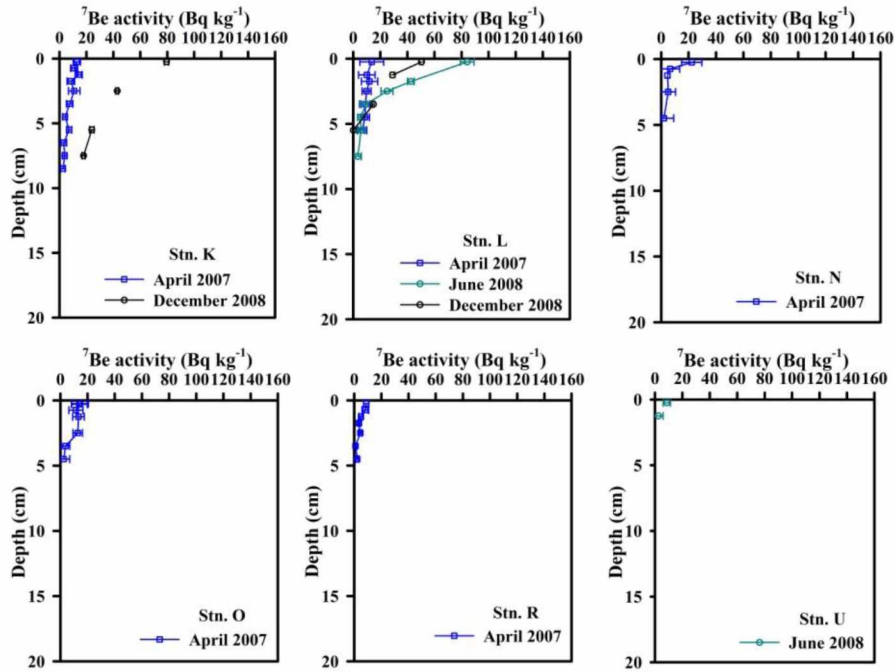


897



898





899

900

901

902

**Figure 3.** Vertical distributions of  $^7\text{Be}$  activities in the sediment cores.

903

904

905

906

907

908

909

910

911

912

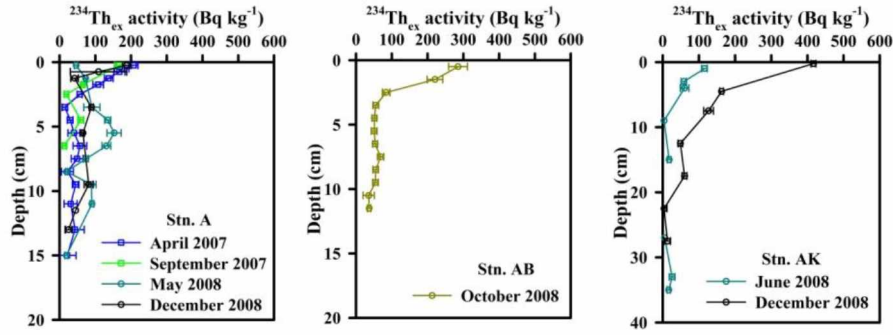
913

914

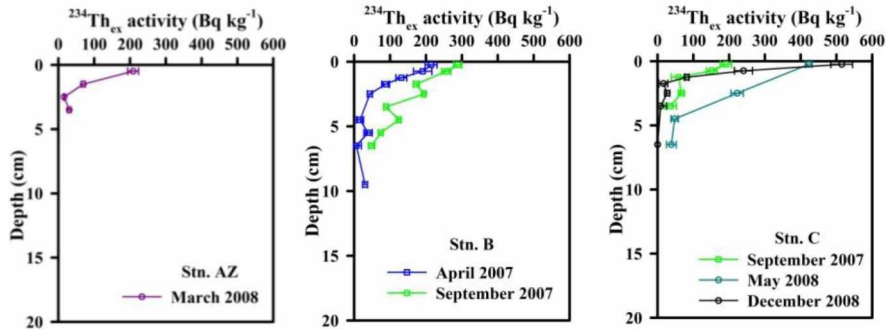
915

916

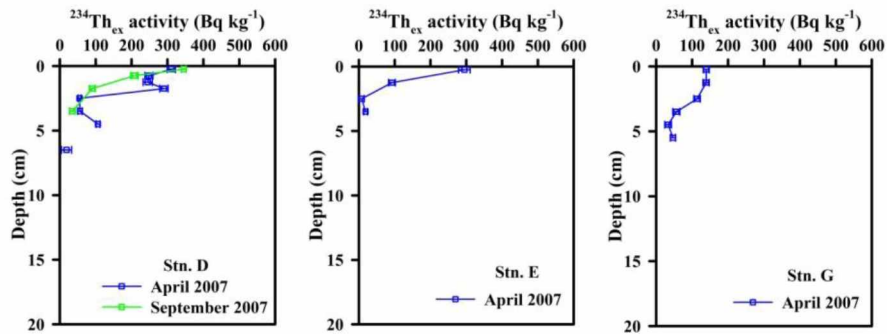
917



918



919



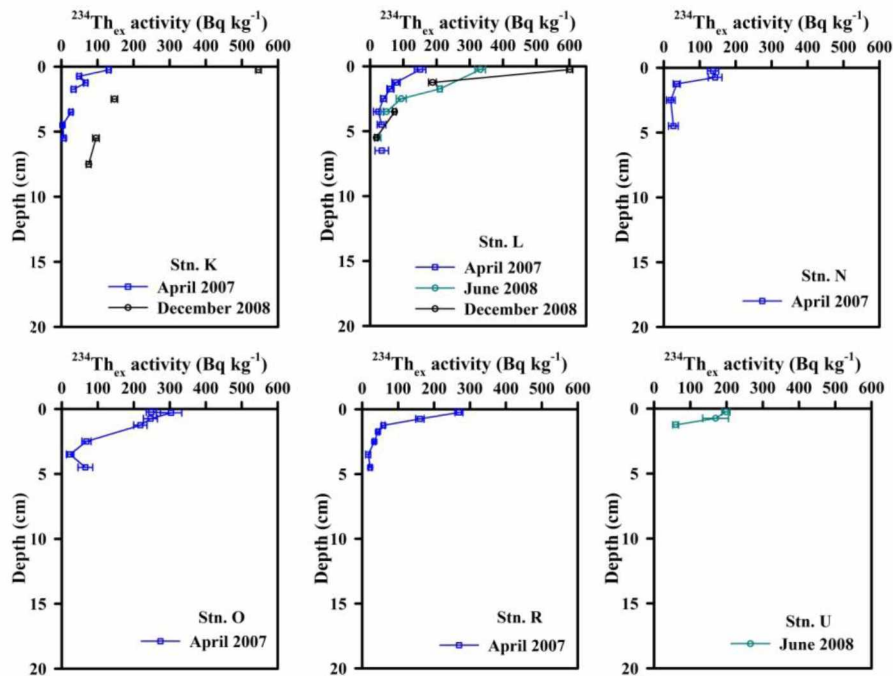


Figure 4. Vertical distributions of  $^{234}\text{Th}_{\text{ex}}$  activities in the sediment cores.

920

921

922

923

924

925

926

927

928

929

930

931

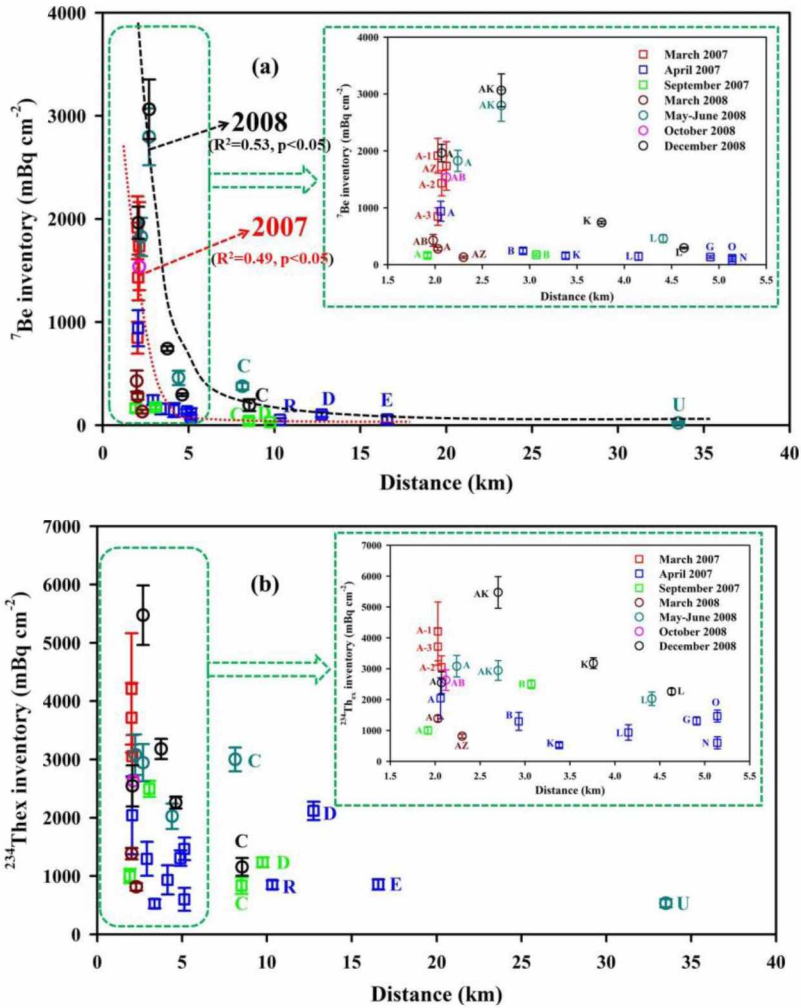
932

933

934

935

936



937

938

939

940

941

942

943

944

945

**Figure 5.** Inventories of  $^7\text{Be}$  (a) and  $^{234}\text{Th}_{\text{ex}}$  (b) in the sediment cores, as a function of distance off the Rhône River mouth for March 2007 (red empty squares), April 2007 (blue empty squares), September 2007 (green empty squares), March 2008 (dark red empty circles), May-June 2008 (dark cyan empty circles), October 2008 (purple empty circles) and December 2008 (black empty circles). The exponential decreases of the  $^7\text{Be}$  inventories with distance in 2007 and 2008 are plotted to highlight the trends.

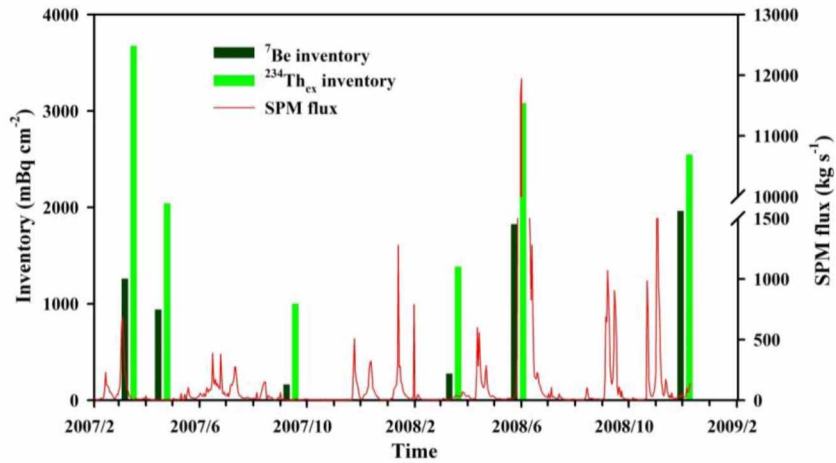
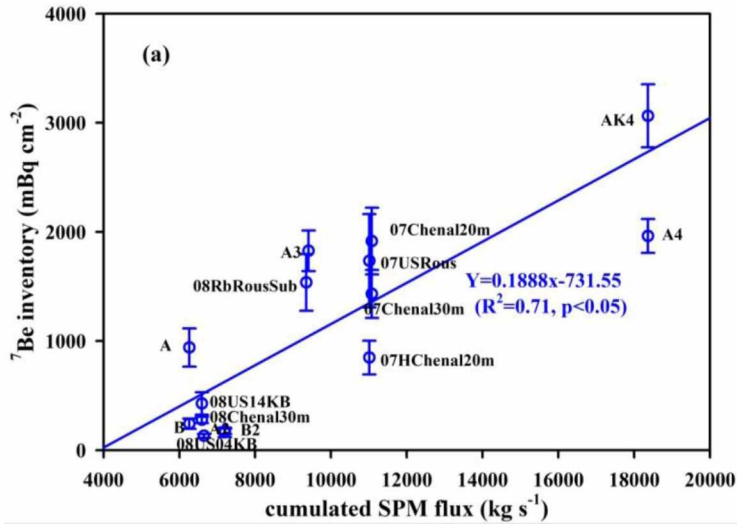
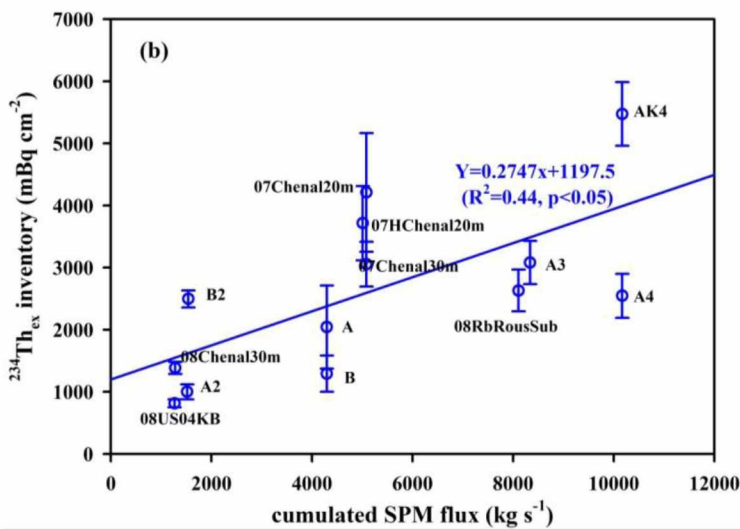


Figure 6. Temporal variations of  ${}^7\text{Be}$  and  ${}^{234}\text{Th}_{\text{ex}}$  inventories at Stn.A.

946  
 947  
 948  
 949  
 950  
 951  
 952  
 953  
 954



955



956

957

958

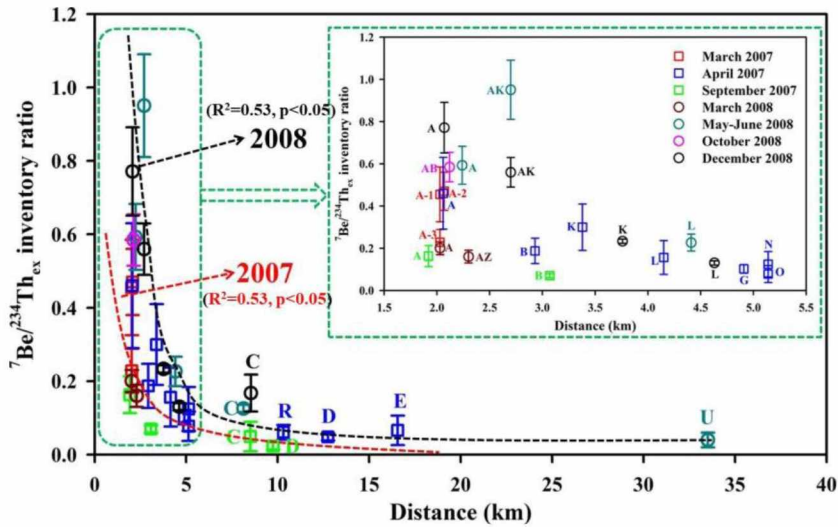
959

960

961

962

**Figure 7.** Relationship between  ${}^7\text{Be}$  inventories in the Rhône River pro-delta and cumulated SPM fluxes calculated over 106 d (2 half-lives of  ${}^7\text{Be}$ ) before the sampling date (a) excluding the Stn.AK3 collected in May-June 2008 flood; and relationship between the  ${}^{234}\text{Th}_{\text{ex}}$  inventories in the Rhône River pro-delta and cumulated SPM fluxes calculated over 48 d (2 half-lives of  ${}^{234}\text{Th}$ ) before the sampling date (b) excluding Stn.AK3.



964

965

**Figure 8.**  ${}^7\text{Be}/{}^{234}\text{Th}_{\text{ex}}$  inventory ratio in sediment cores as a function of distance from the

966

Rhône River mouth for March 2007 (red empty squares), April 2007 (blue empty

967

squares), September 2007 (green empty squares), March 2008 (dark red empty

968

circles), May-June 2008 (dark cyan empty circles), October 2008 (purple empty

969

circles) and December 2008 (black empty circles). The exponential decreases of

970

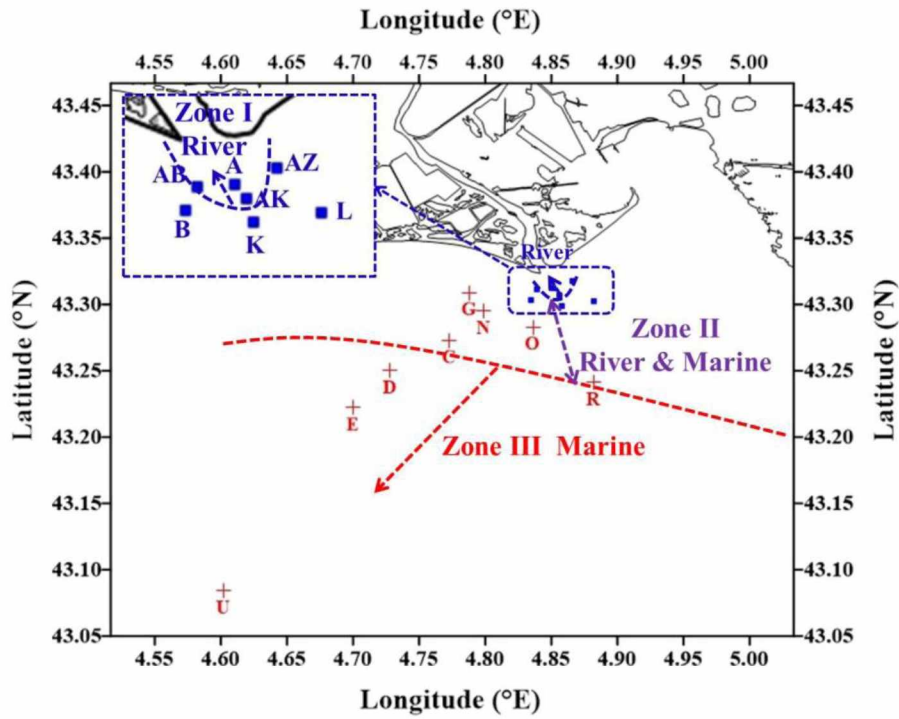
${}^7\text{Be}/{}^{234}\text{Th}_{\text{ex}}$  inventory ratios with distance off the Rhône River mouth in 2007 and

971

2008 are plotted to highlight the trends.

972





973  
 974  
 975  
 976  
 977  
 978  
 979  
 980  
 981  
 982  
 983  
 984

**Figure 9.** The zonation with different dominant sources of particles: input of river-borne particles (River) near the river mouth and marine particles (Marine) on the continental shelf.

**Table 1. Sample information from selected stations of the Rhône River pro-delta sediments**

Stations	Samples	Lat. (°N)	Long. (°E)	Depth (m)	Collection date (dd-mm-yyyy)	Measurement length (cm)	Distance (km) <sup>±1</sup>	Inventory	Data from Lab	
Southwest transect (SW)										
A	2007Chenal20m(-1)	43.311	4.853	28	13-03-2007	16	2.03	closed	IRSN/LMRE	
	2007Chenal30m(-2)	43.313	4.855	27	13-03-2007	16	2.07	closed	IRSN/LMRE	
	2007HChenal20m(-3)	43.311	4.851	28	15-03-2007	14	2.03	closed	IRSN/LMRE	
	A	43.312	4.852	25	20-04-2007	16	2.06	closed	LSCE/LSM	
	A2	43.313	4.851	19	13-09-2007	7	1.92	closed	LSCE/LSM	
	2008Chenal30m	43.313	4.854	26	16-03-2008	15	2.03	closed	IRSN/LMRE	
	A3	43.310	4.851	32	29-05-2008	16	2.24	open	LSCE/LSM	
	A4	43.313	4.855	21	04-12-2008	12	2.07	open	LSCE/LSM	
	AB	2008US 14KB	43.312	4.835	26	16-03-2008	6	2.08	open	IRSN/LMRE
		2007US-Rous	43.310	4.841	27	15-03-2007	6	2.12	closed	IRSN/LMRE
	2008RbRousSub	43.310	4.842	27	11-10-2008	13	2.12	closed	IRSN/LMRE	
AK	AK3	43.307	4.856	42	08-06-2008	38	2.70	closed	LSCE/LSM	
	AK4	43.307	4.856	46	04-12-2008	30	2.70	closed	LSCE/LSM	
AZ	2008US 04KB	43.318	4.866	25	15-03-2008	4	2.30	closed	IRSN/LMRE	
B	B	43.303	4.836	56	20-04-2007	10	2.93	closed	LSCE/LSM	
	B2	43.302	4.834	56	12-09-2007	7	3.07	closed	LSCE/LSM	
G	G	43.309	4.788	48	27-04-2007	6	4.91	closed	LSCE/LSM	
N	N	43.295	4.799	67	24-04-2007	5	5.14	closed	LSCE/LSM	
C	C2	43.272	4.772	75	14-09-2007	4	8.51	closed	LSCE/LSM	
	C3	43.274	4.776	75	30-05-2008	7	8.13	closed	LSCE/LSM	
	C4	43.273	4.770	72	04-12-2008	7	8.54	closed	LSCE/LSM	
D	D	43.250	4.728	74	23-04-2007	8	12.75	closed	LSCE/LSM	
	D2	43.301	4.728	72	14-09-2007	4	9.75	closed	LSCE/LSM	
E	E	43.222	4.700	75	21-04-2007	5	16.56	closed	LSCE/LSM	
U	U3	43.084	4.602	90	02-06-2008	1.5	33.51	closed	LSCE/LSM	
South transect (S)										

K	K	43.301	4.858	62	29-04-2007	9	3.38	closed	LSCE/LSM
	K4	43.296	4.852	67	03-12-2008	8	3.76	open	LSCE/LSM
O	O	43.283	4.836	79	24-04-2007	5	5.14	closed	LSCE/LSM
R	R2	43.241	4.882	98	28-04-2007	5	10.32	closed	LSCE/LSM
Southeast transect (SE)									
L	L	43.304	4.880	64	19-04-2007	7	4.15	closed	LSCE/LSM
	L3	43.303	4.883	65	01-06-2008	8	4.41	closed	LSCE/LSM
	L4	43.300	4.883	66	07-12-2008	6	4.63	closed	LSCE/LSM

986 a) This indicates the distance from the sampling station to the reference site (43.329°N, 4.842°E) in the Rhône River mouth.

987

988

989

**Table 2. Inventories of  $^7\text{Be}$  and  $^{234}\text{Th}_{\text{ex}}$  in the Rhône River delta sediment cores and their  $^7\text{Be}/^{234}\text{Th}_{\text{ex}}$  inventory ratios**

Stations	Samples	Collection date (dd-mm-yyyy)	Cumulated SPM flux over 106 d ( $\text{kg s}^{-1}\text{d}^0$ )	Cumulated SPM flux over 48 d ( $\text{kg s}^{-1}\text{d}^0$ )	$^7\text{Be}$ inventory ( $\text{mBq cm}^{-2}$ )	$^{234}\text{Th}_{\text{ex}}$ inventory ( $\text{mBq cm}^{-2}$ )	$^7\text{Be}/^{234}\text{Th}_{\text{ex}}$ inventory ratio
Southwest transect (SW)							
A	2007Chenal20m(-1)	13-03-2007	11080	5082	1915±306	4209±954	0.45±0.13
	2007Chenal30m(-2)	13-03-2007	11080	5082	1432±221	3055±362	0.47±0.09
	2007HChenal20m(-3)	15-03-2007	11013	5008	847±155	3715±597	0.23±0.06
	A	20-04-2007	6265	4296	940±175	2042±668	0.46±0.17
	A2	13-09-2007	7197	1518	163±43	1001±121	0.16±0.05
	2008Chenal30m	16-03-2008	6593	1281	277±29	1385±98	0.20±0.03
	A3	29-05-2008	9408	8336	1826±186	3081±348	0.59±0.09
	A4	04-12-2008	18364	10168	1963±155	2546±353	0.77±0.12
AB	2008US 14KB	16-03-2008	6593	1281	428±103	-	-
	2007US-Rous	15-03-2007	11013	5008	1735±428	-	-
	2008RbRousSub	11-10-2008	9350	8108	1537±260	2630±336	0.58±0.07
AK	AK3	08-06-2008	63216	59652	2797±275	2944±319	0.95±0.14
	AK4	04-12-2008	18364	10168	3064±289	5474±512	0.56±0.07
AZ	2008US 04KB	15-03-2008	6647	1268	130±18	814±65	0.16±0.03
B	B	20-04-2007	6265	4296	242±47	1294±292	0.19±0.06

	B2	12-09-2007	7204	1541	173±25	2496±137	0.07±0.01
G	G	27-04-2007	6101	895	134±21	1308±131	0.10±0.02
N	N	24-04-2007	6205	2169	74±23	599±196	0.12±0.06
C	C2	14-09-2007	7183	1496	41±32	837±142	0.05±0.04
	C3	30-05-2008	12919	11629	377±33	3000±204	0.13±0.01
	C4	04-12-2008	18364	10168	194±57	1156±153	0.17±0.05
D	D	23-04-2007	6215	2860	102±24	2118±159	0.05±0.01
	D2	14-09-2007	7183	1496	29±10	1237±83	0.02±0.01
E	E	21-04-2007	6268	3698	56±38	856±89	0.07±0.04
U	U3	02-06-2008	47852	45699	21±11	535±69	0.04±0.02
South transect (S)							
K	K	29-04-2007	5949	901	157±53	525±77	0.30±0.11
	K4	03-12-2008	18352	10149	741±23	3181±173	0.23±0.01
O	O	24-04-2007	6205	2169	113±51	1465±193	0.08±0.04
R	R2	28-04-2007	6052	712	52±15	850±76	0.06±0.02
Southeast transect (SE)							
L	L	19-04-2007	6278	3879	146±68	934±250	0.16±0.08
	L3	01-06-2008	35895	34019	459±70	2026±218	0.23±0.04
	L4	07-12-2008	18518	10352	294±13	2261±102	0.13±0.01

990 a) The cumulated SPM fluxes are calculated over 106 d (2 half-lives of  $^7\text{Be}$ ) before the sampling date.

991 b) The cumulated SPM fluxes are calculated over 48 d (2 half-lives of  $^{234}\text{Th}$ ) before the sampling date.

992

993

994

**Table 3.** Zoning in the Rhône pro-delta, where influences between river-borne particles and marine particles are dominant

Zone	Distance (km)	$^7\text{Be}/^{234}\text{Th}_{\text{ex}}$ inventory ratio	River vs. Marine
I	< 3.0	>0.50	River
II	3.0–8.5	0.10–0.50	River & Marine
III	>8.5	<0.10	Marine

995